

NASA Technical Memorandum 58215

10 MAY 1980  
NASA

Colorimetric Principles as Applied  
to Multichannel Imagery

Richard D. Juday

JULY 1979

25 SEP 1979  
MCDONNELL DOUGLAS  
RESEARCH & DEVELOPMENT LIBRARY

NASA

M79-16553

VHSA-111-00213

NASA Technical Memorandum 58215

# Colorimetric Principles as Applied to Multichannel Imagery

Richard D. Juday  
*Lyndon B. Johnson Space Center*  
*Houston, Texas*



National Aeronautics  
and Space Administration

**Scientific and Technical  
Information Branch**

1979

TABLE OF CONTENTS

Section	Page
1. INTRODUCTION . . . . .	1
2. SURVEY OF THE LITERATURE . . . . .	3
3. MULTISTIMULUS VALUES, ANGULARITY, AND CHROMATIC FIDELITY . . . . .	11
4. THE PROJECTION-ADDITION MODEL . . . . .	23
5. DEMONSTRATION OF A CHROMATIC DEFECT IN CONVENTIONAL COLOR IMAGE GENERATION . . . . .	33
6. MATCHING DATA SPACE TO COLOR SPACE . . . . .	41
7. NUMERICAL VALUES IN THE PROJECTION-ADDITION MODEL FOR THE JOHNSON SPACE CENTER FR-80 . . . . .	47
8. IMAGERY PRODUCED BY UCS TRANSFORMATIONS . . . . .	53
9. CONCLUSIONS . . . . .	59
ABBREVIATIONS AND SYMBOLS . . . . .	61
REFERENCES . . . . .	65

## TABLES

Table		Page
7-1	CALCULATION OF LIGHT TABLE CHROMATICITY COORDINATES . . . . .	48
7-2	CALCULATION OF CHROMATICITY COORDINATES FOR THE THREE FILM PRIMARIES . . . . .	49
7-3	LINEAR FIT TO FILM DENSITY VS. INPUT COUNTS . . . . .	50
7-4	TRISTIMULUS VALUES OF LIGHT TABLE AND FULLY ACTIVATED INDIVIDUAL PFC CHANNELS . . . . .	50
7-5	MATRIX ELEMENTS FOR EQUATION (4.7), THE INVERSION FROM COLOR SPACE TO INPUT COUNTS . . . . .	51
7-6	CONVERSION BETWEEN (L*a*b*) AND (X,Y,Z) . . . . .	52

## FIGURES

Figure		Page
2.1	Block diagram showing relationships between control vector $\underline{J}$ (derived from data values) and the resultant color vector $\underline{U}$ . . . . .	8
3.1	CIE color-matching functions . . . . .	12
3.2	Idealized spectral responsivity curves for a four-band MSS . . . . .	13
3.3	Lines of constant protanopic chromaticity in the normal diagram (from Judd and Wyszecki, 1963) . . . . .	15
3.4	Hypothetical angularity diagram shown embedded in two-dimensional data space . . . . .	17
3.5	Arrows indicate a constant-angularity transformation . . . . .	18
3.6	Original data space . . . . .	18
3.7	Data space transformed to accentuate a region, while retaining angularity . . . . .	18
3.8	Angularity shift resulting from a simple bias . . . . .	20
5.1	Point distribution in constant-total-density plane . . . . .	35
5.2	One hundred points cast randomly into a constant-total-density plane, distributed among three primaries, and converted to chromaticity. As the range $\Delta D$ of optical density available to each primary increases, a larger chromaticity range is accessible, but the points bunch toward the primaries. (See text for further discussion.) . . . . .	39
6.1	Matching data envelope to color gamut . . . . .	43
6.2	Product UCS-4, in which the line of soils is coincident with the gray axis and development of vegetation canopy is in the negative- $\eta$ chromatic direction. Note the unused, but accessible, portion of color space in the positive- $\eta$ direction . . . . .	45

Figure		Page
8.1	Method used to display a saturated color . . . . .	54
	Color plate 1 . . . . .	57
	Color plate 2 . . . . .	58

## 1. INTRODUCTION

The objective of this work is the false-color display of numerical imagery, using colorimetry to quantify and refine the process. The term "false color" denotes either that the displayed color for a datum need bear no resemblance to what would have been seen by an unaided eye, or else that a color assignment is made to a quantity that has no inherent color inasmuch as an eye would have no response to the quantity. Mathematical descriptions of color vision are used to preserve information and relationships with as little distortion as possible in moving from the original numerical data to a color image. The operations to be performed on data prior to their conversion to color are quantified.

A simplistic model of the colorimetry of a particular color image generating machine is constructed from measurements. The model is used to demonstrate quantitatively stated principles in the production of examples of imagery derived from satellite data. Future refinements to both the colorimetric model and to data processing prior to image generation are described.

Existing literature is discussed in section 2; this section includes references to the standard nomenclature and literature, with which the reader is assumed to be familiar. Section 3 contains an elaboration on the rationale for relating data values to colors. Section 4 describes the colorimetric model and how simple measurements allow its mathematical construction. Section 5 demonstrates a defect common to conventional generation of color images from numerical data. Section 6 shows practical methods of using known characteristics of data distributions and color gamuts to produce the linear mappings between data and color. Section 7 gives examples of the computations for a particular color image generating machine. Section 8 discusses the sample imagery. Abbreviations and symbols are listed for the reader's convenience just prior to the references.

The author wishes to acknowledge the substantial support that has been given this project by others. Mr. M. C. Trichel was the chief technical sounding board for most of the ideas presented here; his cautious criticism and clear thinking have been very valuable. Dr. J. F. Paris provided a knowledge of related work. Mr. R. M. Carver performed most of the measurements that went into the colorimetric model. Mr. Carver also converted the author's algorithms into an easily useable computer program. Mr. F. Johnson did many of the computer graphics that gave knowledge of the color gamut.

**Page intentionally left blank**

**Page intentionally left blank**

## 2. SURVEY OF THE LITERATURE

Multichannel imagery is a two-dimensional set of points (the object space) with a vector of  $n$  dimensions (lying in the data space) being a function of position in the object space. The conventional color photograph is a familiar example; the angular coordinates in front of the camera lens comprise the object space, and the densities of the three dyes in the emulsion layers represent the data space. Other examples include X-ray pictures, in which the data space has a single dimension, and census figures, in which demographic information has many dimensions (population density, average age, number of telephones per household, length of residence, country of national origin, etc.). Particular application is made in this paper to remotely sensed earth resources data, in which images of the earth's surface are made in terms of physical variables. The examples employed are primarily from multispectral scanner (MSS) data, in which spectral radiance from the instrument's instantaneous field of view is integrated to give an  $n$ -dimensional vector, the radiance in each of the  $n$  bands.

Photographic and colorimetric terminology is used herein without extensive explanation. Nimeroff (1968) and Wyszecki and Stiles (1967) are recommended as references for the colorimetric terminology and Eynard (1973) for the photographic terminology. The reader would well be familiar with tristimulus values, color-matching functions, uniform chromaticity scale (UCS) transformations, chromaticity and chromatic coordinates, the Maxwell triangle, reflection color solid, associated color temperature, and additive and subtractive color (all colorimetric terminology) as well as with the Hurter and Driffield (H&D) curve; reciprocity; interimage effects; saturation; masking; transmittance factors; and spectral, analytical, and equivalent neutral densities (all photographic terms). Familiarity with an MSS system such as that of Landsat (General Electric, n.d.) would be helpful but is not required.

In the field of remote sensing of earth resources, many data are put into false-color imagery; i.e., two-dimensional pictures are made in which the visual appearance is governed by attributes of the remotely sensed scene but in which the appearance is not at all similar to what the naked eye would see. In one sense, the "false" nature of the imagery is an inescapable consequence of the extension of remote sensing to wavelength regimes to which the eye does not respond. Only for a sensor that duplicates (or nearly so) the eye's response can "true color" imagery be produced. The goal of true-color standard photography is also vigorously pursued (MacAdam, 1967) of course; but here we shall be concerned with machine generation of color from numerical control inputs as an existing process, describing the relationship between control inputs and color outputs, and inverting the relationship to discover the control values to produce a desired color.

Many fields other than remote sensing of earth resources use the generation of false-color imagery from two-dimensional maps of multi-dimensioned data. Examples include display of count rates from X-ray telescopes viewing solar flares, tomography, and even noninstrumental cases such as the display of demographic variables (e.g., median population age or time of a county's maximum population) or other physical variables (e.g., temperature or altitude) in map form. In the field of earth resource remote sensing, data are taken by MSSs, both from aircraft and spacecraft. (An MSS produces digital data, the numbers being proportional to the mean radiance in each of several spectral bands, at points in a grid of directions in the scanned space.) Because the sensitivity of the scanners may extend beyond the region of the eye's spectral sensitivity, color displays of the data will necessarily be false color as mentioned earlier. With this realization comes the lifting of a considerable mass of restrictions. For example, we are freed from having to get flesh tones "right". Since the image is certainly not going to depict the scene as an unaided eye would see it, we are free to apply rational processes to the image generation. Section 3 elaborates the author's thoughts on appropriate rational processes.

Various methods of making color imagery from numerical imagery exist: computer-driven television; ink-jet plotters; machines in which cathode-ray-tube (CRT) displays are imaged directly onto color film; and film registration, in which black-and-white transparencies, individually modulated by numerical information, are sequentially printed in registration onto a color master. Specific examples of each type, in the same order, are General Electric's Image 100, the CalComp ink-jet plotter, Information International's FR-80, and the standard method of making the color images from the Landsat data at the NASA Goddard Space Flight Center (Polger, 1973). Of those techniques, the television screen directly driven by computer is colorimetrically the cleanest; light from one of the primaries (red, green, or blue gun) is directly added to light from another (when the eye is far enough from the screen to be unable to resolve the individual phosphor dots). In contrast, the photographic process is less clean; the illumination source forms part of the colorimetric description. Even more complicated are the ink systems, which being color subtractive (Judd and Wyszecki, 1963) in operation, are computationally tractable until the colored dots begin to overlap; at that point, the color-subtractive process becomes very complex in comparison to a color-additive process.

The photographic color processes have essentially the same colorimetry among themselves. A principal departure from color additivity is found in the interimage effect (Pearson, 1973). In a color-negative film, blue light activates principally the yellow-forming dye layer, but to a lesser extent the magenta- and cyan-forming layers as well. Typically, less interimage communication occurs from red light onto the yellow and magenta and from the green onto the yellow and cyan, but in precise colorimetry those are also considered (Wallis, 1975). "Masking" (Pearson, 1973) is a well-known technique for compensating for much interimage effect in photographic reproduction. The logarithmic nature

of the H&D curve (density plotted against logarithm of exposure) is another departure from strict additivity.

Installed at the NASA Lyndon B. Johnson Space Center is an FR-80 color image generating machine manufactured by Information International, Inc. The machine is known as the production film converter (PFC). It is used to convert numerical data into color imagery; input is in the form of digital counts ranging from 0 to 255 in each of three channels, and output is exposed color film which is developed into positive transparencies.

The UCS space is a three-dimensional color space. An abbreviated statement of the quality of a UCS space is that a difference of one unit of geodesic distance is, under optimum viewing conditions, just barely perceptible to the average-eye viewer (Wyszecki and Stiles, 1967). For the most part, units are not given; however, following MacAdam (1942) and others, the unit of distance may be taken as a just noticeable difference (JND). The mathematical description of a UCS space depends on large bodies of experimental data, and line element theory (Wyszecki and Stiles, 1967) is involved in an accurate formulation. A consistent feature exists in the bodies of data--that despite color vision's being three dimensional, the UCS space cannot be embedded in a three-dimensional Euclidean space because of its having negative Gaussian curvature (Wyszecki and Stiles, 1967). It being computationally simpler to operate in a space in which the distance measure is simply the Euclidean metric, many attempts (summarized as of 1971 by Friele, 1972) have been made to find an acceptable approximation having a Euclidean metric to describe color differences. The International Illumination Committee<sup>1</sup> (CIE, 1976) has adopted the (L\*a\*b\*) system as an approximation to the UCS space within the reflection color solid for D<sub>65</sub> illumination (i.e., within the gamut of color experiences that can be produced by manipulating the spectral reflectance distribution of a surface illuminated by an irradiance simulating daylight with an associated color temperature of 6500 K). In the present work, the (L\*a\*b\*) space will be regarded as having a UCS. See section 7 for the (L\*a\*b\*) formulation.

The PFC is presently configured so that the transmission density (McCamy, 1973) in each of its three channels--red, green, and blue--is a linear function of the control level input to that channel, with zero input to the other two channels. (Transmission density is the logarithm of the ratio of flux within the wavelength passband of the densitometer, with and without the sample's being present in the light beam.) Inter-image effects are not considered in the present setup, although to some extent they are taken into account in the structure of the measurements made in the process of density linearization. According to the Weber-Fechner law, density linearization for a single channel provides visually uniform spacing along the path traced out in color space. That law

---

<sup>1</sup>Commission Internationale de l'Eclairage.

states that to be just noticeably brighter, one patch of light must exceed in luminance that of another by a constant fraction (Judd and Wyszecki, 1963, p. 310). However, when more than one channel is activated, the PFC (as presently configured) is no longer a uniform chromaticity machine. Modeling the three-color behavior of the PFC allows the writing of an interface algorithm that will cause the PFC to simulate a UCS condition. With this interface, numerical data transformed by rotation, common scale factors in all three dimensions, and bias, will have color differences that are in proportion to their Euclidean separation in the original feature space. Considerable flexibility in the process of generating color imagery with controlled characteristics is thus indicated. The production of actual examples is shown.

Two highly interesting approaches are aligned closely with this work. Pratt (1978) and Wallis (1975) describe a process in which a compensation unit is numerically designed to minimize some desired error functional between desired and actual tristimulus values in a photographic system. A more direct route, founded in the physics of the film process, is described at length by Wallis (1975) and more briefly by Pratt (1978); it is associated with severe computational problems in the inversion of colors to control inputs.

In another related work, Faugeras (1976) derives his own approximation to a UCS space and performs manipulations in it. His goal is fidelity in color reproduction within the photographic process and in image transmission.

In the most strongly allied work found in the literature, Taylor (1974) explicitly maps from a data space into an approximation to a UCS space. He notes that optimal mappings may vary from discipline to discipline, drawing guidance for the transformations from covariance matrices of scenes having interest for the individual disciplines. He takes the logarithm of data values, with the intent of removing the effect of changes in illumination on the relative spectral values. Taylor cites his logarithmic transformation as having foundation in information theory. Indeed, logarithms abound in information theory; for example, Kullback (1968) defines the logarithm of the likelihood ratio of a measurement as the information for discrimination in favor of one hypothesis over another. Note that this is the logarithm of the likelihood ratio for the measurement and not the logarithm of the ratio of the measurements themselves.

A substantially larger body of measurements is required to generate the compensation units of Wallis (1975) than is required for the simpler model of this work. In addition to providing a simpler analytically invertible model of the control input to color output process, this author explores the rationale of color image generation from remotely sensed data from a phenomenological standpoint. Pratt (1978) and Wallis (1975) do not consider the generation of imagery as a complete process beginning with numerical data having no natural color and ending with an

analyst's attempt to visualize the meaning of the data through the windowpane of the color generation process.

Faugeras (1976) seeks fidelity in color reproduction; he does not attempt the use of colorimetry to show an analyst the numerical structure of his data.

Taylor (1974) does not maintain strict orthogonality in his mappings between data space and color space. In visually displaying the logarithm of data values without similarly transforming the values before machine analysis, the analyst of the visual imagery and a machine performing numerical work on the data have different metrics on the same data. Relative differences between data vectors will have differing magnitudes as interpreted by image analyst and computer. Proportionality between the metrics for image analyst and computing machine is a goal of this research.

If one wishes to remove the effects of both illumination variation and atmospherically induced radiation propagation variations, logarithmic transformation of data values remains to be shown to be of similar effect to available correction procedures, rooted in the physics of the problem and in phenomenological behavior of Landsat data (Lambeck et al., 1978). In the transformations shown in this work, the simplest physical model is employed for compensation of illumination variation (Lambert's law, assuming diffuse surface feature reflection). That technique satisfactorily maintains the balance of the data within the expressible color range without distorting proportional relationships among the components of the data vector. No atmospheric corrections are made by Taylor or by this author; if such are to be done as part of machine analysis, they should also be applied to the visually displayed data.

Until likelihood ratio and data measurements are connected through physics or phenomenology, it is improper to assume that the logarithm of a measurement is proportional to the information it contains. As a final point of departure between this work and Taylor's, Taylor gives no description of his colorimetry. As is made evident later, numeric control of color generation is complex, and Taylor gives no guidelines for its achievement and verification. This paper gives a numerical model, describes supporting measurements, and outlines a set of verification/correction measurements for a more highly refined work.

In agreement with Taylor (1974), the author considers a UCS system as the appropriate coordinates in which to discuss the color of a point transformed from data to color. In the approximations used here, the Euclidean metric is roughly proportional to visual discriminability. For large (more than 10 or 20 JNDs) color differences, the  $(\mathcal{L}, j, g)$  coordinate system is preferable to the  $(L^*a^*b^*)$  system, the latter being designed principally for accuracy with respect to small color differences. The  $(\mathcal{L}, j, g)$  system was constructed on a grid of large color differences (MacAdam, 1974). However, the use of either system is an advance over most of the methods of color generation that have been used

previously; and the  $(L^*a^*b^*)$  system has the property of being analytically invertible, which is a great convenience in finding the control inputs to produce a desired color. Further work could include developing an economical inversion for the  $(\mathcal{L}, j, g)$  system.

The model of the colorimetry of the PFC is used to provide an interface between the PFC and the independent channels of information that are extracted from the data. The model allows the PFC to simulate being a uniform chromaticity machine with respect to control inputs. This situation is graphically indicated in figure 2.1.

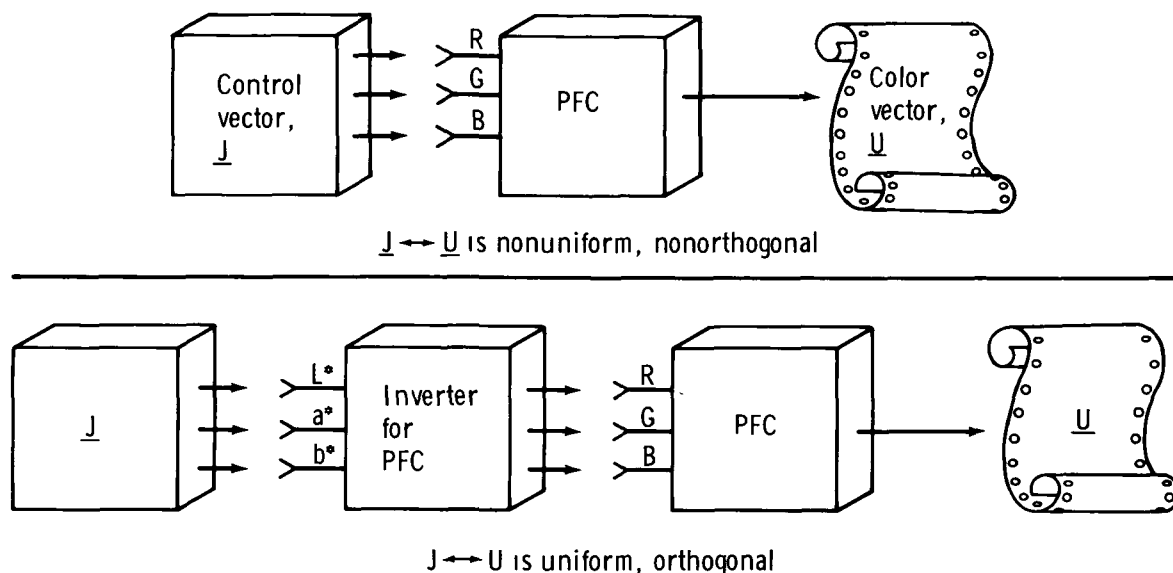


Figure 2.1. Block diagram showing relationships between control vector  $\underline{J}$  (derived from data values) and the resultant color vector  $\underline{U}$ .

The goals of this research have been to examine the principles of generating color imagery from numerical multichannel data, to include quantitative colorimetry in the considerations, and to model the colorimetry of a particular color image machine to allow accommodation of the principles to the production of optimum imagery. The principles are put into quantitative form as follows:

1. Budgeting of the color range accessible to a generalized color-making machine is to be optimized with respect to the range of the data being represented in the imagery.

2. Visual discriminability (between the colors mapped into by two data vectors) is to be in proportion to some variable of interest, that variable being a metric on the data space.

3. Colorimetry offers a vector space in which (at least locally) the axes visually are orthogonal and have the same mutual scale. The mapping from data space to color space should include manipulations to exploit those characteristics.

4. For a given image interpretation problem, one may wish a sequence of types of transformations from data space to color, in whose sequence there is a refinement of the metric. That is, data may be sequentially modified before being transformed into color in a manner designed to replace more and more of the image analyst's work by numerical manipulation. The ultimate, and likely unreachable, goal is a classification map in which all of the analyst's work is done by machine. The sequence would be iteratively determined by quantification of the information being used by the analyst per intuition and training.

Following these principles, one develops a set of transformations under the projection-addition model. Based on existing models of the statistical behavior of agricultural areas in Landsat data (Kauth and Thomas, 1977), film products with the following properties are described:

1. A product (UCS-1) with maximal chromatic expansion, that parameter having dimensions of JNDs per input count.

2. A product (UCS-2) with a constant relationship between Landsat counts and color, so that as the overall location of a body of data shifts in feature space, the shift will be visible as a change in the overall chromatic appearance of the transparency.

3. A product (UCS-3) in which the major variations of data in feature space are presented as chromatic changes, i.e., an isoluminous product.

4. A product (UCS-4) in which soils typically will fall along the gray axis, with vegetation cover causing chromatic departure from gray.

Examples of the first two products are shown and are examined for general compliance with the principles. Methods for verifying the accuracy of the colorimetric model are described, and further work that could be based on this project is outlined.

### 3. MULTISTIMULUS VALUES, ANGULARITY, AND CHROMATIC FIDELITY

Let us consider the nature of multichannel data and how it relates to color vision. This seems to be a natural thing to do, since both Landsat and our eyes look at the earth and respond to radiometric energy and since it has been amply demonstrated that the eye can recognize earth features when Landsat data are properly presented in false color.

To begin with a bold statement: There is no natural color in Landsat MSS data. There is, to be sure, natural color in the radiant energy to which Landsat responds; and using metameric presentation,<sup>2</sup> one can attempt to match the color of an image manufactured from Landsat data to the color of the radiant energy that activated the satellite. In his sections 16.4 through 16.7, Pratt (1978) discusses the general procedure. However, because the mechanisms by which the satellite and the eye respond to radiation are so substantially different, any color presentation of Landsat data to the eye is a false-color presentation.

The origin of a chromatic diagram for the eye is in the color-matching functions. Color vision is three dimensional, for three parameters--e.g., the tristimulus values--completely specify the color experience from any arbitrary spectral distribution of radiant energy. The color-matching functions are the kernels with which the radiant spectrum is integrated to give the tristimulus values:

$$\underline{T} = \int_{\lambda} \underline{t}(\lambda') L_{\lambda}(\lambda') d\lambda' \quad (3.1)$$

where

$$\underline{t} = \begin{pmatrix} \bar{x} \\ \bar{y} \\ \bar{z} \end{pmatrix}$$

---

<sup>2</sup>Color stimuli of identical tristimulus values but of different spectral energy distributions. All color photography uses this principle (Wyszecki and Stiles, 1967, sec. 3.9).

is the vector of CIE tristimulus distribution coefficients,  $\underline{T}$  is the vector of tristimulus values

$$\underline{T} = \begin{pmatrix} X \\ Y \\ Z \end{pmatrix}$$

and  $L_\lambda$  is the spectral radiance. The chromatic coordinates  $x$  and  $y$  are formed from the tristimulus values by normalizing  $X$  and  $Y$  to the sum of the tristimulus values.

$$\left. \begin{aligned} x &= \frac{X}{X + Y + Z} \\ y &= \frac{Y}{X + Y + Z} \end{aligned} \right\} \quad (3.2)$$

The triad  $x,y,Y$  is equivalent in content to the triad  $X,Y,Z$ . As indicated in the form of equation (3.1), when lights are combined by the addition of their spectral radiances, the tristimulus values of the individual lights add directly (fig. 3.1).

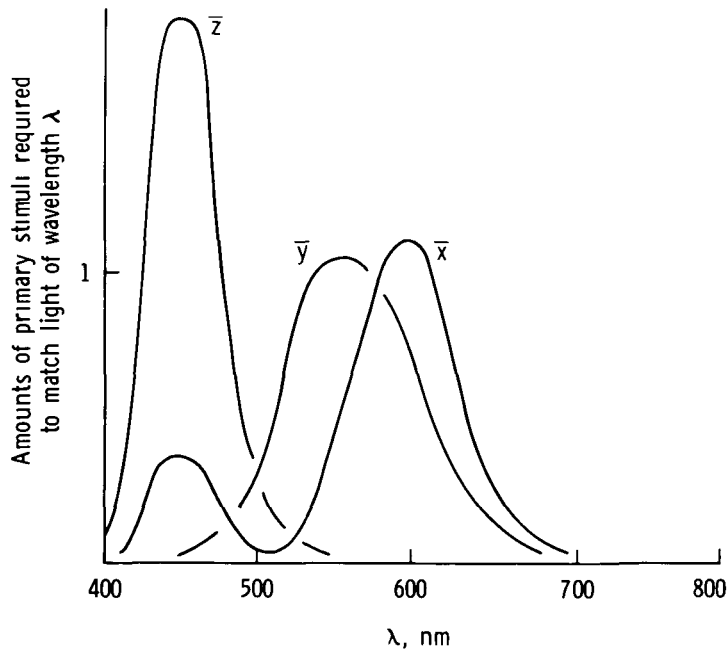


Figure 3.1. CIE color-matching functions.

When a monochromatic light is swept through the visible spectrum, the chromatic coordinates trace out the spectrum locus, a curve enclosing the chromatic coordinates of all color sensations that the eye can have.

Consider now the MSS's analog of the chromaticity diagram. Assume that the MSS has some ideal characteristics such as nonoverlapping square passbands and, in each channel, zero responsivity to wavelengths outside its passband. These characteristics are exemplified in figure 3.2.

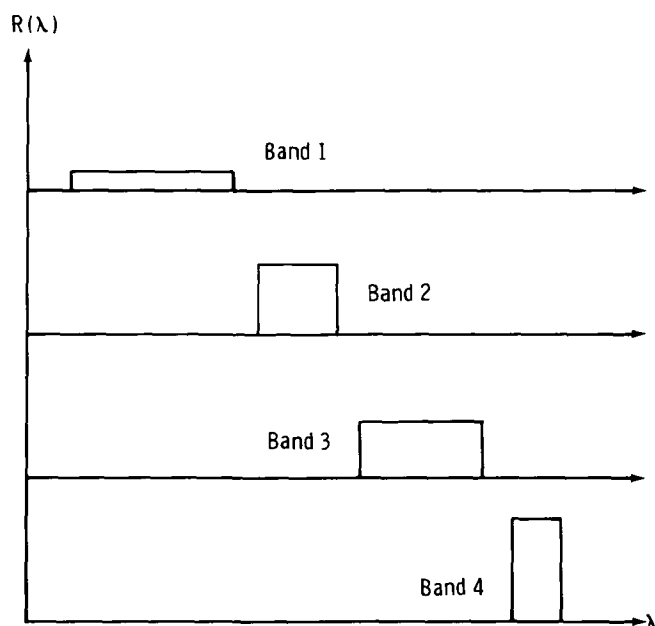


Figure 3.2. Idealized spectral responsivity curves for a four-band MSS.

A set of primaries numbering the same as the number of channels is necessary and sufficient to stimulate the MSS to reproduce any naturally occurring set of counts. One primary is required for each channel; any set of count values for the channels is achieved by independent adjustment of the primaries. ("Independent" here means that the adjustment of one primary does not affect the count value in the unassociated channels.) Given the square passband, the primary for a channel can be equally well chosen anywhere in the wavelength passband of that channel. Now, when the total range of wavelength sensitivity of the instrument is swept with monochromatic light, the color-matching functions that derive are simply the familiar charts of the spectral bandpass of the individual channels.

In the production of a chromaticity diagram for the eye, the dimensionality of the response was reduced by one by normalizing to (i.e., dividing by) the sum of the tristimulus values. This was somewhat arbitrary; a weight could have been applied to each of the tristimulus values, with an associated rearrangement of the chromaticity diagram. Indeed, this is the basis for transforming between tristimulus values for various sets of primaries (Wyszecki and Stiles, 1967; sec. 3.3). For the MSS analog of a chromaticity diagram, two such normalizations come to mind: normalization to the responsivity of the channel and normalization to the noise in the channel. For specific applications, other weighting factors could apply, e.g., correlations of the channels with a feature of interest. By one means or another, normalizing to a function of all the channel values reduces the dimensionality of the remaining information to give the MSS analog of chromatic information. In normalization to each channel's noise level, the eliminated quantity is the quanta of signal in the measurement. The resulting analog of a chromaticity diagram will be tailored by the choice of weight values. Differing weight values will only distort a presentation in the "chromaticity diagram"; they will not make fundamentally different diagrams.

We will refer to the reduced information as "angularity," which corresponds to chromaticity for the eye. The terms "color" and "chromaticity" are reserved herein for descriptions of actual perceptions. Angularity is the proportionality of a data point's distribution among the channels. In a multidimensional space, one can describe the direction to a point by the angles it makes with the coordinate axes, hence, the term angularity.

For wavelengths falling within no passband, the MSS's multistimulus values (to coin a term in analog to the eye's tristimulus values) are all zero. Just as in the case of the eye, if there is no [visible light detectable energy], there is no [chromaticity angularity] either. So for such wavelengths, there are no corresponding points on the MSS angularity diagram. They just do not exist.

For a wavelength falling within only one of the passbands, the multistimulus values are all zero except for the channel activated by the light. After normalization and dimension reduction, the angular coordinates are found to be all zero except for the activated channel, and its value is unity. Thus the spectrum locus for the MSS is highly discontinuous in comparison to the one for the eye, consisting only of the points at unity on each of the independent chromatic axes. For nonmonochromatic activation of an n-band MSS, the accessible portion of angularity space for nonnegative multistimulus values (volts in the channels) is the locus of all vectors  $(f_1, f_2, \dots, f_n)^T$  restricted by

$$0 \leq f_i \leq 1$$

and

$$\sum_1^n f_i = 1.$$

Angularity diagrams of further reduced dimensions can be expressed by normalizing the original  $n$  channels to functions of more than one argument (the arguments themselves being independent functions of multi-channel values), or in equivalent fashion, by sequentially reducing the dimensionality of angularity diagrams. Methods would have to be rooted in the physics of particular instances; a visual analog (see fig. 3.3) is describing the chromaticity diagram for a visually defective person in terms of the angle measured about the protanope's confusion point in the standard CIE chromaticity diagram (Wyszecki and Stiles, 1967, p. 406). (The protanope is a member of one class of dichromatic color defective viewer; a dichromat requires only two primaries to match any color. When plotted in the normal CIE chromaticity diagram, loci of constant chromaticity for a dichromat are approximately radial from a confusion point. The protanope, as shown in fig. 3.3, cannot distinguish red from green; the deuteranope and the tritanope are characterized by different confusion points from that of the protanope.)

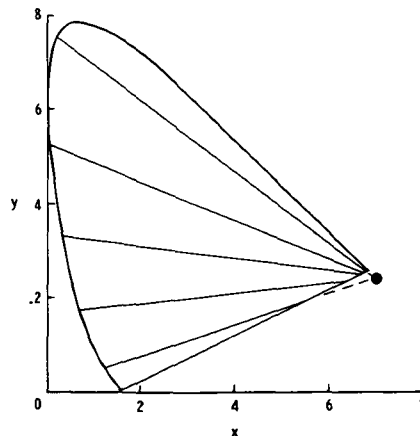


Figure 3.3. Lines of constant protanopic chromaticity in the normal diagram (from Judd and Wyszecki, 1963).

In the case of a two-band MSS, the angularity coordinate is the (weighted) proportion of the activation of the MSS that appears in either one of the channels; the range of angularities is the line from zero to one on the single angularity axis. The nonangular information is the (weighted) total of the two channels' outputs.

Consider the matter of wavelength discrimination in the comparison of MSS and eye. The MSS just propounded can determine in which of

n channels a monochromatic wavelength appears, but not where within that channel. For Landsat, the wavelength discrimination divides its sensed spectrum into four parts. The eye, however, has much finer wavelength discrimination. It can discriminate several tens of monochromatic wavelengths. The eye, however, is not equivalent to an MSS with several tens of channels; it has only three channels. The apparent dilemma is resolved by noting that the eye's color-matching functions overlap and individually are not constant functions of wavelength. As a monochromatic light activates two of the color-matching functions, the ratio of the tristimulus values gives wavelength information. MSSs are typically designed toward having nonoverlapping square spectral responsivities.

The eye can discriminate among several million chromatic and brightness combinations. With one more channel than the eye has, the MSS might be thought to be able to discriminate among even more. That is, in addition to having three channels to match the eye, the MSS has another channel to take on its own values to contribute to finer discrimination. However, we have not yet sufficiently characterized the model MSS to settle this issue. Suppose that MSS is so coarsely digitized that only two outputs are possible in each channel. Then there are discriminable only  $2^n$  different regions of the measurement vector space. However, merely increasing the number of levels to which the MSS's detectors are digitized will not guarantee that discriminability increases in proportion. Under several simplifying assumptions (linearity, independence of channels when viewed instrumentally, digitization at, or finer than, the noise level, etc.), the number of meaningful levels that can be presented by a channel is the range of the channel divided by the noise. In the conversion of multichannel imagery to color imagery, this must be kept in mind. If the noise in the measurement is given too much chromatic expansion (by being scaled along with the signal in the measurement), it will have an exaggerated visual impact. If a channel having a substantial natural range of signal to noise is expressed as one chromatic coordinate and its signal-to-noise range is so great as to suppress the data noise below the visual discrimination threshold, then in expressing another channel onto the orthogonal chromatic coordinate, its noise level should also be kept at or below the visual threshold. In this generalization, the term "signal" carries the nonstandard connotation of "meaningful information" rather than the restricted "counts in a channel" definition. A channel might be given a greater-than-unity weight, for example, on account of its importance to a particular identification problem in assigning a "signal" value to its number of counts.

The availability of measurement vector space is no guarantee that naturally occurring data will fill all its corners. Landsat MSS data acquired over agricultural regions, for example, are observed to lie in a rather restricted, almost planar subspace of the four-dimensional space having counts in the channels as basis vectors. The fundamental problem in the presentation of color imagery from multichannel imagery is the matching of the data space to the eye space. Obviously, only occupied portions of data space need to be mapped into eye space, so

that any clustering of data will be considered in a most efficient mapping from data space into eye space. The mapping need not carry unoccupied portions of data space into realizable portions of color space.

In the generation of color imagery from Landsat MSS data, attempts have been made to create transformation from feature space to the control inputs of the PFC that would have the previously elusive quality of "chromatic fidelity". The concept of chromatic fidelity is easily expressible in the colorimetry terminology we have developed. Chromatic fidelity amounts to a mapping from the sensor's angularity diagram into the eye's chromaticity diagram that is independent of levels in the data channels. In other words, loci of constant angularity in data space map into loci of constant chromaticity in color space. Additionally, the ratio of incremental angularity change to incremental chromaticity change is independent of location in chromatic and data space. (The essential problem is then to find the color space that has the desirable metric by which to measure chromaticity change.) Operations that leave a data point stationary in the sensor's angularity diagram will leave it stationary in the eye's chromaticity diagram, if chromatic fidelity exists. If a data-to-eye transformation is equivalent to an independent mapping from angularity diagram to chromaticity diagram, it retains chromatic fidelity. As an example, a constant multiplicative factor applied to all data channels does not affect the proportion of total counts in a channel and so has no effect on angularity. A simple bias, however, affects a channel's proportion of the total and so alters a point's position in the sensor's angularity diagram. Take the two-channel sensor as an example. The sensor's angularity diagram (fig. 3.4) amounts to a line showing the proportion of the total counts in each of the two channels.

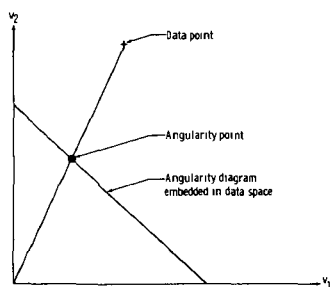


Figure 3.4. Hypothetical angularity diagram shown embedded in two-dimensional data space.

Transformations in the data space that move data points along radii from the origin are angularity-fidelity transformations (fig. 3.5):

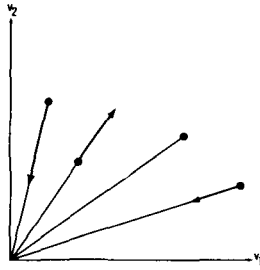


Figure 3.5. Arrows indicate a constant-angularity transformation.

The indicated transformation retains angularity characteristics; it is easily seen that considerably more flexibility than a multiplicative scaling is possible. To accentuate a region of the data space while retaining angularity fidelity, consider the transformations in figures 3.6 and 3.7:

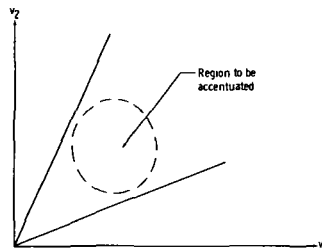


Figure 3.6. Original data space.

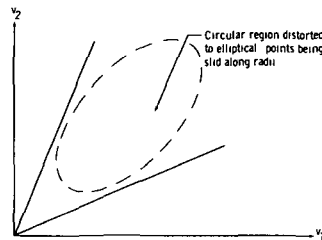


Figure 3.7. Data space transformed to accentuate a region, while retaining angularity.

If a bias is distributed among the coordinates of a point in proportion to those coordinates, then no angularity shift results. If  $g$  designates the gain and  $b$  the bias, the values of channels 1 and 2 can be altered:

$$v_1' = g \cdot \left[ v_1 + b \cdot \frac{v_1}{v_1 + v_2} \right]$$

$$v_2' = g \cdot \left[ v_2 + b \cdot \frac{v_2}{v_1 + v_2} \right]$$

and it is easily verified that

$$\frac{v_1}{v_2} = \frac{v_1'}{v_2'}$$

so that the angularity is maintained. The upshot is that a bias can be included in a linear angularity fidelity transformation from feature space to PFC input if the gain and bias are included in the form:

$$v_i' = g \cdot v_i \cdot \left[ 1 + \frac{b}{\sum_j v_j} \right]$$

Nonlinear transformations of this type are achieved if

$$v_i' = g \left( \sum_j v_j \right) \cdot v_i \cdot \left[ 1 + \frac{b \left( \sum_j v_j \right)}{\sum_j v_j} \right] \quad (3.3)$$

which can be written

$$v_i' = v_i \cdot f \left( \sum_j v_j \right) \quad (3.4)$$

In equations (3.3) and (3.4),  $f$ ,  $g$ , and  $b$  are functions. In particular, note that  $f$  can be negative for some values of  $\sum_j v_j$ .

Note that a data point can be moved through the origin to negative values--presumably saturating at zero counts--while being slid along a

radius. This is a feature unattainable with a constant multiplicative factor and demonstrates the additional flexibility available.

In figure 3.8, the angularity effect of a simple bias is apparent.

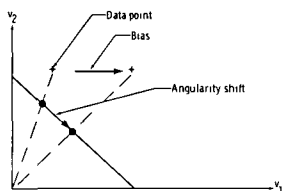


Figure 3.8. Angularity shift resulting from a simple bias.

What color is Landsat data? Actually, Landsat data are just numbers and numbers do not have color. You can map numbers into a color space, however, and do so in a fashion designed to meet certain criteria. One such criterion, alluded to earlier in this section, is to attempt the duplication of the color that was present in the original radiance field that the satellite observed. Because of substantial differences in the visual process and the MSS's process of number generation and the associated angularity diagram, there is not a radiometrically deterministic route to do that for an arbitrary original scene. You can set about the job in ad hoc way, though. Since healthy vegetation shows up brightly in the near-infrared channels of Landsat and since healthy vegetation is most often green visually, you can make the association from channel 4 of the Landsat to a visually green phosphor on a television tube. (Keep in mind that it is not for radiometrically valid reasons.) Since we are dealing with false color in any circumstance, one is entirely free to set up new constraints on color imagery generation. Those constraints may well take forms other than a requirement for resemblance to aerial photographs, and there is a fertile field for discussion on the constraints. Considerably more flexibility is offered by colorimetry theory than by assignments of channels to permutations of guns, selection of biases, and linear scaling factors. The following are offered as germinal suggestions.

1. An approximation to a UCS space is the proper representation of the visual process, in matching multichannel data to the eye. The CIE tristimulus values are convenient for mathematical manipulations since they add linearly, but the eye has nonuniform response to motions in the associated chromaticity diagram. In a UCS system, visibility of chromatic motions is directly proportional to their Euclidean distances. In using a UCS space, one is assured that manipulations performed in data space will be exactly tracked in perceptibility. This feature allows attention to be placed on the behavior of data in the data's own space. Worry about the complicated mutual involvement of changing gun count biases (which has a chromatic side effect) and linear scalings of channels (which have perceptibly differential effects from gun to gun) is

eliminated. If a feature warrants a larger visual range, its volume in data space can be expanded in full confidence that its visual impact will be increased in proportion.

2. Scatter plots of typical (agricultural) scenes should be matched with appropriate cross sections of the accessible portions of the UCS space to perform the mapping of the multichannel imagery into visual imagery. The noise level in the multichannel data should not greatly exceed the visual discrimination threshold, except for special effect (e.g., classification maps).

3. For some purposes, a single transform from Landsat data space to eye space should be sought to limit the number of products on which an analyst will have to train.

4. At different times of a crop year, different portions of the Landsat data space may be nonlinearly transformed to occupy larger volumes in the data space. The accentuated portions of Landsat space should be examined for overlap into the same regions of visual space, so that as an accentuated feature is tracked through data space, it will continue to move in visual space.

5. Consistent with the limitations of suggestion no. 2, the data variability should be aligned with the visual space axes in such an order that the greatest data variability will be along the longest visual axis, etc. This may also fall under the requirement that some semblance of natural interpretative mechanisms be maintained; brightness of the image perhaps ought always to be proportional to the total (weighted) output of the MSS.

6. The "contouring" effect of limiting the number of levels of display should be reconsidered after transformation to a UCS. If contouring is desired, it should be introduced in the UCS coordinates rather than in the CIE or color gun cube coordinates. This would be in accordance with suggestion no. 1, in which the eye is considered to have its representation in the UCS space.

7. The light tables used with the film directly affect the appearance of the imagery, and there is notable difference among them. The qualities of the light table are an input to any UCS transformation (and indeed, to any quantitative assessment of film/analyst performance). The light table should be standardized where possible. Bulbs that have high relative output in the blue are readily available, and the blue is a potentially very productive region for the extension of the accessible portions of the UCS space. In order to see variations in blue transmission, blue illumination must naturally be present. Room illumination spectrum should match that of the light table to give a single illumination spectrum to which the analyst is to adapt.

8. An origin about which to measure angularity may well not correspond to the zero-count origin. The measurement vector corresponding to

zero reflectance at the ground is a philosophically pleasing origin; that vector will correspond to a finite radiance because of atmospheric path radiance. If fundamental interest is in ground reflectance rather than in atmospherically modified radiance, satellite or aircraft data should be standardized against atmospheric variations prior to other operations. Instrumental biases also enter into consideration of a center for angularity.

9. A caveat: Colorimetric theory can improve the visual presentation of imagery but cannot let the analyst see things that are not present in feature space or that are masked by noise, etc. One cannot do better than his original data's fundamental quality.

#### 4. THE PROJECTION-ADDITION MODEL

The model of the color generation process used for this work is called the "projection-addition model". It is believed to be original, although it has roots extending as far back into color photography as Maxwell's famous 1861 lecture, in which he projectively added transparencies. In a sense, this present projection-addition model is a revival of additive color photography (Wallis, 1975, p. 84). It regards the result of exposing the PFC's color reversal film to the three activating primaries to have the same appearance as would individually exposing three images (one for each exposing primary) and then projecting the three into registry so that their tristimulus values add directly.

The projection-addition model is technically accurate for a color television display; in this instance, lights from the phosphor dots add directly if viewed from a distance large enough that individual dots are not visually resolved. (For CRT display, linearization in density in what follows is replaced by linearization in logarithm of radiance of the phosphor dots.) In film displays, interimage effects cause a certain amount of crosstalk, with the result that the projection-addition model is not strictly applicable. Because the model's supporting measurements are made with all dye layers having been exposed to the activating light, though, at least some of the interimage effects may be anticipated to have been incorporated into the model. Methods of compensating for interimage and other effects are described later in this section. In applying the model to the film process, one appeals to the fact that color film pictures of natural scenes and portraits, for example, are entirely recognizable to the eye. The distortions in color between natural scenes (with the uncontrolled spectral nature of their radiance) and the photographs of the scenes surely exceed the color variations found in the projection-addition model, with its constant spectral irradiance sources for exposing the film. Surely the results are also of higher color fidelity than those that would be obtained by photographing a television screen modulated according to the model. It is expected that even the method of photographing a television screen would give transparencies with color qualities recognizably in agreement with those desired. Finally, displaying the PFC control tapes on a color television monitor gave appearance consistent with the film's. Later in the section, measurements that can be used to verify the colorimetry of applying the model to the film system are described. Those measurements can also be used for calculating corrective feedback into the film model.

Measurements apropos to the projection-addition model are described, and the model is formulated. Two distinct paths to higher-order approximations are pointed out. The relative advantages of the

projection-addition model are discussed, analytical invertibility being the most attractive advantage.

The film is assumed to have certain classical characteristics, including reciprocity, operation in the linear portion of the H&D curve, and concentration-independent spectral behavior of the dye layers' transmittance factor (McCamy, 1973, and Pratt, 1978). Verification of the operation in the linear portion of the H&D curve is indicated from the measurements made for the projection-addition model. As a matter of fact, a lookup table within the PFC causes a relationship between input counts and density that is more highly linear and extends further than the typical H&D curve relating density to log exposure.

The formulation of the projection-addition model is expressed simply in matrix and vector form, as follows:

$$\begin{pmatrix} X \\ Y \\ Z \end{pmatrix} = \begin{pmatrix} X_R & X_G & X_B \\ Y_R & Y_G & Y_B \\ Z_R & Z_G & Z_B \end{pmatrix} \begin{pmatrix} a_R \\ a_G \\ a_B \end{pmatrix} \quad (4.1a)$$

or

$$\underline{T} = \mathbb{P} \underline{a} \quad (4.1b)$$

in which  $\underline{T}$  is the vector of tristimulus values,  $\mathbb{P}$  is a matrix of primary tristimulus values, and  $\underline{a}$  is a vector giving the activations of the red, green, and blue color channels. The activation  $a_j$  of the  $j$ -th channel is defined as the ratio of the transmittance factor to its maximum value;  $a_j$  ranges from  $a_{j,\min}$  to 1 as the  $j$ -th channel input is varied from minimum to maximum. Derivation of the elements of the model follows.

The PFC functions by imaging a black-and-white television screen through color filtration onto color reversal film. The color channel is determined solely by which filter is in place. The film, after sequential exposure to the colored images, is given standardized development. There is rigid control over the interplay of the operating curve of the CRT, the film sensitometry, and the development chemistry. The purpose of the control is for uniform reproduction of colors from given inputs; the process is regarded as stable for the purposes of this model. Control inputs for each channel range from zero counts to 255 counts in one-count increments.

The transmittance factor is determined individually for the channels by standard densitometric measurements. The densitometer is filtered to measure light at wavelengths near the peak of the film's spectral transmittance factor for the given color channel, and the illumination/collection geometry is set up to simulate the conditions of film viewing by analysts (diffuse illumination/specular collection). The transmittance factor is the ratio of fluxes received at the detector with and without the film's being present in the densitometer. The quantity transmission density is the logarithm (base 10) of the transmittance. For the reader's (and the writer's) convenience, these quantities will be shortened to "transmission" and "density"; where appropriate, the adjective "spectral" is appended to denote "wavelength dependent".

For each channel independently activated, the transmission was measured for all 256 control inputs. Each channel was found to be linear in density to a satisfactory approximation--i.e., the combination of CRT operating curve (governed by a lookup table), film sensitometric curve, and color filtration simulates the classical H&D situation.

Next, it was noted that simultaneous activations of all three channels at identical input levels produced visually achromatic grays, with full activation of all channels producing functionally clear film.

Spectral transmission measurements were conducted on film patches produced at full activation of individual channels. As mentioned above, an assumption of the projection-addition model is that this curve does not change in shape but only by a wavelength-independent factor as the activation of the gun changes.

Finally, spectral radiance measurements of the light table were taken. The light table forms the reference illumination for the colorimetric description. By colorimetric convention, the luminosity of the reference illumination is  $Y_0 = 100$ . The other tristimulus values for the reference illumination are calculated from measurements (or specifications) of the chromaticity  $(x_0, y_0)$  through definition of the coordinates:

$$\left. \begin{aligned} x &= \frac{X}{X + Y + Z} \\ y &= \frac{Y}{X + Y + Z} \end{aligned} \right\} \quad (3.2)$$

whence

$$\left. \begin{aligned} Z &= \frac{1 - x - y}{y} Y \\ X &= \frac{x}{y} Y \end{aligned} \right\} \quad (4.2)$$

The chromaticity coordinates for the primary film patches and the light table are calculated as follows:

$$\underline{T}_k = h_k \int_{\lambda} \underline{t}(\lambda') \tau_k(\lambda') L_{\lambda}(\lambda') d\lambda'$$

with  $k = R, B, G, 0$ ;  $\tau_0(\lambda') \equiv 1$ ; and  $h_k$  a normalizing constant that disappears in equation (3.2). The integration is performed over all visible wavelengths and is in practice approximated by summation of products.

$$\underline{T}_k \approx h_k \Delta\lambda' \sum_i \underline{t}(\lambda'_i) \tau_k(\lambda'_i) L_{\lambda}(\lambda'_i)$$

etc.

Equation (4.2), inserted into equation (4.1a) and taken for full activation of all channels, yields

$$100 \begin{pmatrix} \frac{x_0}{y_0} \\ 1 \\ \frac{1 - x_0 - y_0}{y_0} \end{pmatrix} = \begin{pmatrix} \frac{x_R}{y_R} & \frac{x_G}{y_G} & \frac{x_B}{y_B} \\ 1 & 1 & 1 \\ \frac{1 - x_R - y_R}{y_R} & \frac{1 - x_G - y_G}{y_G} & \frac{1 - x_B - y_B}{y_B} \end{pmatrix} \begin{pmatrix} Y_R \\ Y_G \\ Y_B \end{pmatrix} \quad (4.3)$$

Given measurements for all other parameters, the values of the primaries' luminosities  $Y_j$  are specified by equation (4.3). The right side of equation (4.3) then multiplies to give matrix  $\mathbb{P}$  in equation (4.1).

Linearization in density vs. counts leads to a simple form for the activation vector a. Denoting counts J and density D,

$$D(J) = D_{\max} - \frac{J}{255} (D_{\max} - D_{\min})$$

and using the definition relating density and transmission,

$$D = -\log_{10} \tau$$

we obtain

$$\tau(J) = (\tau_{\min})^{1 - \frac{J}{255}} \cdot (\tau_{\max})^{\frac{J}{255}}$$

Defining

$$q \equiv \left( \frac{\tau_{\max}}{\tau_{\min}} \right)^{\frac{1}{255}} \quad (4.4)$$

then subscripting for the three channels and further defining

$$E \equiv \begin{pmatrix} \tau_{R,\min} & 0 & 0 \\ 0 & \tau_{G,\min} & 0 \\ 0 & 0 & \tau_{B,\min} \end{pmatrix} \quad (4.5)$$

and

$$\underline{q}(J) \equiv \begin{pmatrix} [q_R]^{J_R} \\ [q_G]^{J_G} \\ [q_B]^{J_B} \end{pmatrix}$$

we have the form

$$\underline{a} = \mathbb{E} \underline{q}(\underline{J}) \quad (4.6)$$

All together,

$$\underline{T} = \mathbb{P} \mathbb{E} \underline{q}(\underline{J})$$

Since  $\mathbb{P} \mathbb{E}$  turns out nonsingular, the control inputs for a desired tristimulus vector are easily determined:

$$\underline{J} = \underline{q}^{-1} \left[ (\mathbb{P} \mathbb{E})^{-1} \underline{T} \right] \quad (4.7)$$

where  $\underline{q}$  is invertible; see equation (4.6).

A model following the physics of the photographic process more closely than the projection-addition model is presented next. In large part, it follows Pratt (1978) and Wallis (1975). The extremely more complicated nature of the more accurate model will become apparent. As a preliminary, we introduce some terms for use with tricolor film. The PFC uses SO-397 film, a color reversal material. After exposure and development, three layers of dye remain in the film, each layer having its own wavelength dependence of light transmission. The analytical density of a dye layer is the density that would be observed were that layer isolated from the others, spectral density refers to the wavelength dependence of density, and integral density refers to the density of all three dye layers assembled in the film. The three dye layers are cyan, magenta, and yellow; roughly speaking, they remove red, green, and blue light (in respective order) from a transmitted beam. For any one dye layer, if the exact amounts of the other two dyes are added to produce a neutral gray (with respect to transmitting a specified reference illumination), the value of that resulting (gray) density is called the equivalent neutral density (END) for the original dye layer under consideration. Scarpace (1978) and Scarpace and Friedrichs (1978) discuss the multiemulsion densitometry concepts and measurements.

The spectral integral density  $D(\lambda)$  is given by

$$D(\lambda) = e_c(\lambda) \cdot c + e_m(\lambda) \cdot m + e_y(\lambda) \cdot y \quad (4.8)$$

where  $e_i$  represents the cyan, magenta, and yellow spectral analytical densities and  $c$ ,  $m$ , and  $y$  are the ENDS.

Operation in the linear portion of the curve (density plotted vs. input counts) of the color reversal film has

$$\begin{pmatrix} c \\ m \\ y \end{pmatrix} = \begin{pmatrix} K_c \\ K_m \\ K_y \end{pmatrix} - \mathbb{F} \begin{pmatrix} J_R \\ J_G \\ J_B \end{pmatrix} \quad (4.9)$$

with  $\underline{K}$  being the densities of unexposed film,  $\underline{J}$  being the input count vector, and  $\mathbb{F}$  being the interimage sensitivity matrix:

$$\mathbb{F} = \begin{pmatrix} \gamma_{cR} & \gamma_{cG} & \gamma_{cB} \\ \gamma_{mR} & \gamma_{mG} & \gamma_{mB} \\ \gamma_{yR} & \gamma_{yG} & \gamma_{yB} \end{pmatrix}$$

The assumption of no interimage effects would have off-diagonal terms in  $\mathbb{F}$  equal to zero. However, the magenta- and cyan-forming layers are notably sensitive to blue light, so that immediately one has to account for  $\gamma_{mB}$  and  $\gamma_{cB}$  being nonzero. At this point, one may as well continue with the entire matrix. Implicit in this model are the assumptions that density linearity occurs [in the product separation of  $\mathbb{F}$  and  $\underline{J}$ , eq. (4.9)] and that the spectral shape of a dye's transmission is not concentration-dependent [in the product separation of END and spectral analytical density in eq. (4.8)]. The model is determined by a set of measurements on  $D(\lambda, \underline{J})$ . A sufficient number of measurements must be run not only to determine the 12 constants in equation (4.9), but also to sort out the spectral analytical densities in equation (4.8). (The spectral analytical densities are best deduced rather than measured by exposure and development of the separate dye layers because each dye is affected by the presence of the others.) Once  $D(\lambda, \underline{J})$  is known, the tristimulus values for illumination by  $E_\lambda(\lambda)$  are then

$$\underline{T} = h \int_{\lambda} \underline{t}(\lambda') \cdot E_\lambda(\lambda') \cdot 10^{-\left\{ \underline{D}_0^T(\lambda') [\underline{K} - \mathbb{F} \underline{J}] \right\}} d\lambda'$$

with

$$\underline{D}_0^T(\lambda) = \left[ e_c(\lambda) \ e_m(\lambda) \ e_y(\lambda) \right]$$

and with

$$h = \frac{100}{\int_{\lambda} \bar{y}(\lambda') \cdot E_{\lambda}(\lambda') \cdot d\lambda}$$

So it is seen that a more closely physical model is complex indeed. Beyond the level of complexity of the projection-addition model, it involves vector subtraction, the inner product with a wavelength-dependent vector, exponentiation, and integration with a wavelength-dependent scalar. Inversion from colors to counts may be anticipated tedious, and of course, a substantially larger body of measurements must be made to support the second model.

The projection-addition model is thus highly preferable to the physical film model on the basis of computational ease; but for a film system, its accuracy is not as yet measured with respect to conformance with UCS conditions, except along the axes corresponding to single-channel activation.

The model itself gives the foundation for verification measurements. Attention to the model's accuracy is best spread evenly in the UCS space rather than in the PFC input space, for the same reasons advanced earlier in favor of mapping data into the UCS space. Accordingly, verification of off-axis accuracy of the model would begin on an evenly spaced grid of vectors in the model's approximation to the UCS space. The grid of color vectors  $\mathcal{G} = \{G_i: G_i \text{ is on the evenly spaced grid in UCS space}\}$  is inverted to give the grid of control vectors  $\mathcal{J} = \{J_i\}$ , which would then be physically expressed as film patches. Measurements similar to those made on the axes in formulating the model would give the set  $\mathcal{D} = \{D(\lambda, J_i)\}$  of integral spectral densities. Absolute calibration would have to be held in measuring the D's; whereas in formulation of the model, only relative calibration was required. [Recall the disappearance of the normalizing constant in eq. (3.2).] Tristimulus values are then found by

$$\underline{T}_i = h \int_{\lambda} \underline{t} \cdot E_{\lambda} \cdot 10^{-D(\lambda', J_i)} d\lambda'$$

with  $\underline{t}$  having the CIE color-matching functions as components, and the values of  $\underline{T}_i$  are converted to the achieved UCS vectors  $\underline{G}_i'$ . The comparison of  $\underline{G}_i$  and  $\underline{G}_i'$  yields the accuracy of the model. If a smooth functional relationship  $\underline{\Delta}(\underline{G}) \approx \underline{G} - \underline{G}'$  can be found, then  $\underline{\Delta}$  provides the correction of the projection-addition model. In using the grid points  $\underline{G}_i$ , one need not apply weights to the points in minimizing deviations while approximating  $\underline{\Delta}$ ; this is a result of distributing  $\underline{G}_i$  evenly in the UCS space. Behavior of  $\underline{\Delta}$  corresponding to vector bias and scalar multiplication can be deleted without affecting the colorimetric UCS character of the model, because the Euclidean metric is modified by only a constant factor.

**Page intentionally left blank**

**Page intentionally left blank**

## 5. DEMONSTRATION OF A CHROMATIC DEFECT IN CONVENTIONAL COLOR IMAGE GENERATION

In conventional image generation systems, the output of a color channel is typically linearized in optical density (or, with television systems, in logarithm of radiance) with respect to input level. Data values to be displayed in color are then linearly scaled into the range of input and, as a result, into optical density (or log radiance). The result is a chromaticity difference between points that have identical proportions but different levels. (This is simply demonstrated; chromaticity scales linearly with transmission, which scales exponentially with density, which scales linearly with input. It is experimentally observed that in high-contrast systems so arranged, picture elements tend towards saturation at the primaries. We refer to the crowding into the points of Maxwell's triangle as "chromatic jamming".) This changing chromaticity seems less than satisfactory; for example, merely changing the sun angle on a Landsat scene should not change the chromaticity of the display. That is, one might well desire the chromaticity of the color representation of a datum to be invariant with respect to scalar multiplications of that datum. The notion of chromatic fidelity is treated at length in section 3; this section shows quantitatively the existence of the chromatic jamming under conventional color transformations.

Assume an idealized film generation system whose tricolor film densities are independently produced by activation of the three guns, that the system is "grayed" (equal inputs to all guns produces a gray result), and that the minimum density of each of the three primaries is taken as zero by modifying the description of the viewing illumination. Let  $T_i$  be the tristimulus values of the  $i$ -th primary at full activation. Activate the three guns to produce tricolor densities ( $D_1, D_2, D_3$ ). The chromaticity of the result is

$$x = \frac{\tau_1 X_1 + \tau_2 X_2 + \tau_3 X_3}{\tau_1 R_1 + \tau_2 R_2 + \tau_3 R_3}$$

$$y = \frac{\tau_1 Y_1 + \tau_2 Y_2 + \tau_3 Y_3}{\tau_1 R_1 + \tau_2 R_2 + \tau_3 R_3}$$

with

$$R_i = X_i + Y_i + Z_i$$

and

$$\tau_i = 10^{-D_i}$$

For later use, note that

$$\left| dD \right| = \left| \frac{d\tau}{\tau \ln 10} \right| \quad (5.1)$$

If the guns are activated to produce independent uniform distributions in density, let's find the distribution in chromaticity (x,y). Let  $D_{\max}$  be the maximum density for a primary; it is the same in each primary because the system is "grayed". The distribution in  $D_i$  is

$$p(D_i) = \frac{1}{D_{\max}}$$

and using equation (5.1),

$$p(\tau_i) d\tau_i = p(D_i) dD_i$$

$$p(\tau_i) = \frac{1}{\tau_i D_{\max} \ln 10}$$

Thus the distribution in all three transmissions is

$$p(\tau_1, \tau_2, \tau_3) = \frac{1}{\tau_1 \tau_2 \tau_3 D_{\max}^3 \ln^3 10}$$

and it is easily anticipated that the distribution is not going to be uniform in chromaticity.

Let us restrict the activations of the guns so that--

- a. plotted against densities, activations lie on a plane of constant total density; and
- b. activations distribute uniformly in that plane.

See figure 5.1. We can then relate planar distributions in density and chromaticity, rather than relate a three-dimension density distribution to a two-dimension chromaticity distribution.

Constraint (a) has the form

$$D_1 + D_2 + D_3 = D_0 = \text{constant},$$

which is equivalent to

$$\tau_1 \tau_2 \tau_3 = \tau_0 = \text{constant}.$$

Under constraint (b), the number of points  $d^2_m$  lying between  $f_i$  and  $f_i + df_i$  ( $i = 1,2$ ) is

$$d^2_m = A df_1 df_2$$

with  $f_i = D_i/D_0$  (and by previous constraint  $f_3 = 1 - f_1 - f_2$ ). Without loss of generality,  $D_{\min} = 0$ ,  $\tau_{\max} = 1$ . Because

$$D(f) = f \cdot (D_{\max} - D_{\min}) + D_{\min} = f \cdot D_{\max}$$

we have from definitions that

$$\tau(f) = \tau_0 f.$$

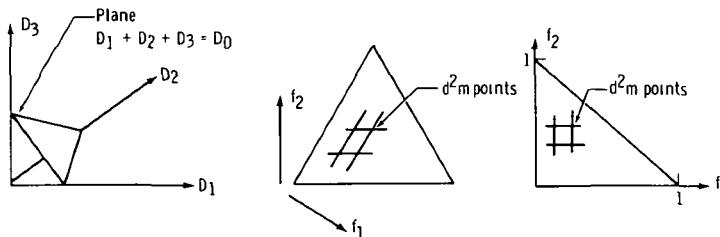


Figure 5.1. Point distribution in constant-total-density plane.

Normalizing so that  $\iint d^2m = 1$  requires  $A = 2$ :

$$\frac{d^2m}{df_1 df_2} = \begin{cases} 2, & (f_1, f_2) \in \Delta \\ 0, & \text{otherwise} \end{cases}$$

where

$$\left\{ (f_1, f_2) \in \Delta \right\} \leftrightarrow \left\{ \left[ 0 \leq f_1 \leq 1 \right] \text{ and } \left[ 0 \leq f_2 \leq 1 \right] \text{ and } \left[ 0 < f_1 + f_2 < 1 \right] \right\}$$

We have  $P(f_1, f_2)$ , the data point density in  $(f_1, f_2)$ . We have also a one-to-one differentiable mapping between  $(f_1, f_2)$  and  $(x, y)$ ,

$$x = \frac{u}{v}, \quad y = \frac{w}{v}$$

with

$$u = \begin{pmatrix} f_1 & f_2 & 1-f_1-f_2 \\ \tau_0 & \tau_0 & \tau_0 \end{pmatrix} (X_1 \ X_2 \ X_3)^T$$

$$w = \begin{pmatrix} f_1 & f_2 & 1-f_1-f_2 \\ \tau_0 & \tau_0 & \tau_0 \end{pmatrix} (Y_1 \ Y_2 \ Y_3)^T$$

$$v = \begin{pmatrix} f_1 & f_2 & 1-f_1-f_2 \\ \tau_0 & \tau_0 & \tau_0 \end{pmatrix} (R_1 \ R_2 \ R_3)^T$$

$$R_i = X_i + Y_i + Z_i$$

Then the density  $Q[x(f_1, f_2), y(f_1, f_2)]$  at the  $(x, y)$  value corresponding to  $(f_1, f_2)$  is

$$Q = p(f_1, f_2) \cdot \text{mod} \begin{vmatrix} \frac{\partial f_1}{\partial x} & \frac{\partial f_1}{\partial y} \\ \frac{\partial f_2}{\partial x} & \frac{\partial f_2}{\partial y} \end{vmatrix}$$

(Sanderson, 1958, p. 11), where "mod" means absolute value of the expression following it.

For  $(f_1, f_2) \in \Delta$ ,

$$Q = 2 \operatorname{mod} \left( \frac{1}{\frac{\partial x}{\partial f_1} \frac{\partial y}{\partial f_2}} - \frac{1}{\frac{\partial x}{\partial f_2} \frac{\partial y}{\partial f_1}} \right)$$

Defining

$$a = \frac{1}{\ln \tau_0} \frac{\partial u}{\partial f_1} = f_1 \left( \tau_0^{f_1 X_1} - \tau_0^{1-f_1-f_2 X_3} \right)$$

$$b = \frac{1}{\ln \tau_0} \frac{\partial u}{\partial f_2} = f_2 \left( \tau_0^{f_2 X_2} - \tau_0^{1-f_1-f_2 X_3} \right)$$

$$c = \frac{1}{\ln \tau_0} \frac{\partial v}{\partial f_1} = f_1 \left( \tau_0^{f_1 R_1} - \tau_0^{1-f_1-f_2 R_3} \right)$$

$$d = \frac{1}{\ln \tau_0} \frac{\partial v}{\partial f_2} = f_2 \left( \tau_0^{f_2 R_2} - \tau_0^{1-f_1-f_2 R_3} \right)$$

$$e = \frac{1}{\ln \tau_0} \frac{\partial w}{\partial f_1} = f_1 \left( \tau_0^{f_1 Y_1} - \tau_0^{1-f_1-f_2 Y_3} \right)$$

$$g = \frac{1}{\ln \tau_0} \frac{\partial w}{\partial f_2} = f_2 \left( \tau_0^{f_2 Y_2} - \tau_0^{1-f_1-f_2 Y_3} \right)$$

results in

$$Q = \frac{2v^4}{(\ln \tau_0)^2} \text{ mod } \left[ \frac{1}{(av - cu)(gv - dw)} - \frac{1}{(bv - du)(ev - cw)} \right]$$

which is clearly not a constant function of  $(f_1, f_2)$ .

Rather than showing analytic values of  $Q$  as a function of  $(x, y)$ , which is even more complicated than this form, we show the results (in fig. 5.2) of casting 100 points at random into the constant-total-density plane and making a scatter plot in the chromaticity triangle. The figure is based on Maxwell's triangle, with saturation at the primaries occurring at the corners and points representing various mixtures of the primaries falling within the triangle. The dependence on  $\tau_0$  shows clearly;  $\tau_0$  and  $\Delta D$  (as the latter is used in fig. 5.2) are related by

$$\tau_0 = 10^{-\Delta D}$$

It is apparent in figure 5.2 that linearization in density requires a balancing act in the selection of the density range, if one is scaling data linearly into density. If a small range of density is chosen, little saturation will occur; a high density difference is required to "turn off" one primary with respect to another. On the other hand, if a large range of density is chosen, there will be a tendency toward the presence of only saturated chromaticities. In the latter event, some pairs of data vectors may be chromatically further separated, but others will be crowded together. Figure 5.2 indicates that even when a balance is struck, the space in the chromaticity triangle is not efficiently utilized.

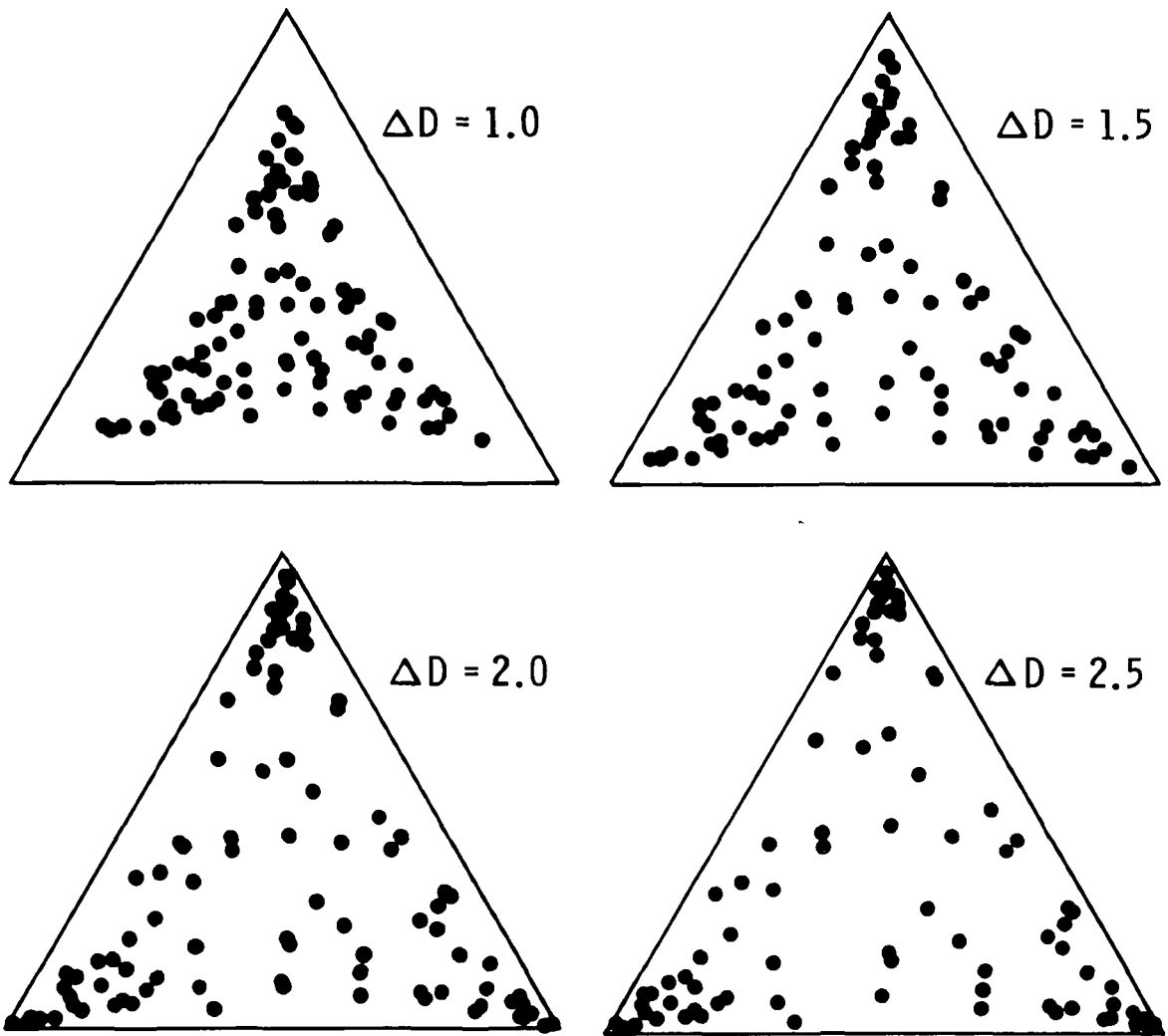


Figure 5.2. One hundred points cast randomly into a constant-total-density plane, distributed among three primaries, and converted to chromaticity. As the range  $\Delta D$  of optical density available to each primary increases, a larger chromaticity range is accessible, but the points bunch toward the primaries. (See text for further discussion.)

This section is not an argument for linearization in transmission. It is intended rather to reinforce awareness of the jamming by showing its analytic basis. As an exercise, Landsat imagery was made with artificially linearized transmission vs. input, so that energy reaching the eye in each primary color was proportional to the energy arriving at the satellite in the associated channel. The imagery was singularly unexciting.

It is interesting to note that the single-channel black-and-white transparencies made from Landsat MSS data are linearized in transmission but that in producing color imagery by compositing the black-and-white imagery onto color film, the 2.0 density range of the black-and-white imagery was compressed "so that visually acceptable prints would be produced" (Polger, 1973). The effect is generally in the direction of compensating for the chromatic jamming shown here, although that process is not quantitatively controlled. An analogy is having a uniformly stretchy rubber ruler, desiring the measuring marks to be placed into coincidence with positions at varying spacing, but being able to pull only at the ends of the ruler.

## 6. MATCHING DATA SPACE TO COLOR SPACE

It is presumed before setting off on the task of matching data space to color space that the worker is familiar with the data and their extent and that the data have been reduced to the point that the quantities to be transformed into color represent no more than three features that are linear and orthogonal with respect to the problem at hand. Some of the operations that might go into such data reduction are standardization with respect to illumination, compensation for atmospheric effects, and projection of multidimensional data vectors onto orthogonal basis vectors chosen for their correlation with specified spectral objects. Extraction of principal components of multidimensional data is another operation that reduces the dimensionality, while retaining the greater part of the variance of the data. Extracting principal components also requires no knowledge of the physics of a situation, which may be a boon in beginning on a problem. At any rate, we presume that the data space being matched to color space has the aforementioned linear and orthogonal characteristics, because insofar as the model and the UCS approximation are valid, the color display will be linear and orthogonal with respect to the three-dimensional input vector.

In addition to knowing the extent of occupied data space, the designer of a transformation should know the gamut of expressible color space. Once the model relating color space to control inputs is established, determination of the gamut is straightforward. In the budgeting of data space and color space with respect to each other, unoccupied data space is best left out of the gamut and occupied data space is best transformed within the gamut, if the goal is large chromatic expansion. For the inevitable data points that do saturate, a choice is to be made about how to express them. That could be to retain chromaticity or to retain brightness or some other criterion. The operation should be performed in the color space if possible rather than in the control input space in order to have the best chance of obtaining the desired expression.

Simply stated, the optimum mapping of data space to color space is the best fit between the occupied portions of data space and expressible portions of color space, under operations of translation, uniform scaling, and rotation. (Those operations retain proportionality of the Euclidean metric in data space.)

Other criteria are secondary. In the accompanying products, the UCS  $L^*$  axis (lightness) was aligned with the brightness direction (positive projection of all channels, lying near the direction of the first principal component) in Landsat MSS data. It was supposed that the analyst would have less problems with training on a product in which objects appearing brighter when viewed directly would also appear lighter.

The next component (containing almost all the remaining variance) was aligned so that the plane containing most of the variance lay in the color space section having largest extent. This gave the largest value of chromatic expansion, JNDs per count. Two types of products are shown. In the first (UCS-1), the transformation was individually determined in the above fashion for each scene; in the second (UCS-2), the envelope of a series of scenes was transformed. The illumination of the individual scenes was corrected by Lambert's law (ratioed by cosine of the solar zenith angle) before being enveloped. There was nonetheless considerably more variation in the enveloped data than in any individual scene, with the result that there was lower chromatic contrast in UCS-2 than in UCS-1. However, UCS-2 had a chromatic consistency missing in UCS-1. As seasons shift, the motion of a scene's extent within the envelope is clearly apparent.

Computationally, the transformation is given by

$$\underline{c} = s \mathbb{R} (\underline{v} - \underline{b}) \quad (6.1)$$

with  $s$  being a scalar,<sup>3</sup>  $\underline{b}$  a bias vector,  $\underline{v}$  the data vector,  $\underline{c}$  the color vector (in  $L^*a^*b^*$  space), and  $\mathbb{R}$  being the appropriate rotation matrix. A rotation matrix is characterized by

$$\mathbb{R}^T = \mathbb{R}^{-1}$$

$$|\det \mathbb{R}| = 1$$

Angles are preserved under multiplication by a rotation matrix; such a matrix is also called an orthogonal matrix.

The elements of equation (6.1) are derivable from a fairly small set of controls. Specifying that  $\underline{c}_1$  is to match  $\underline{v}_1$  and  $\underline{c}_2$  is to match  $\underline{v}_2$  entirely determines  $s$  and also constrains  $\mathbb{R}$  and  $\underline{b}$ . Specifying a UCS plane by mentioning  $\underline{c}_3$  (noncollinear with  $\underline{c}_1$  and  $\underline{c}_2$ ), and specifying on which side of the line through  $\underline{c}_1$  and  $\underline{c}_2$  a third point  $\underline{v}_3$  is to lie within the plane, leaves only the reflection through the  $(\underline{c}_1, \underline{c}_2, \underline{c}_3)$  plane as a free variable. Specifying on which side of the  $(\underline{c}_1, \underline{c}_2, \underline{c}_3)$  plane the

---

<sup>3</sup>The scalar  $s$  is the chromatic contrast, having dimensions [colors per count], or in general [colors per input unit].

point  $\underline{v}_4$  is to fall entirely determines equation (6.1). Note that forcing  $\underline{c}_i$  into conjunction with  $\underline{v}_i$ ,  $i = 1, 2, 3$ , gives a solution to equation (6.1), except for the reflection, but does not guarantee rotation character for the derived  $\mathbb{R}$ . In deriving values for  $s$ ,  $\underline{b}$ , and  $\mathbb{R}$ , the designer must take care not to overspecify.

Let us run briefly through an example, illustrated in figure 6.1.

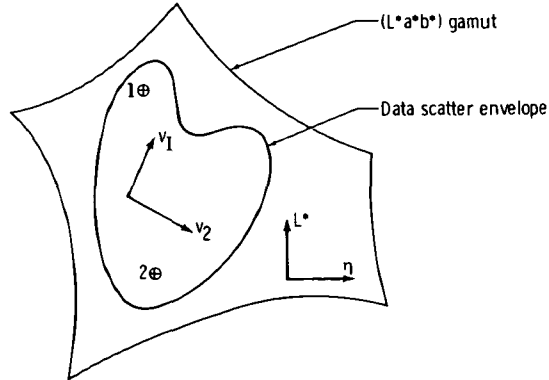


Figure 6.1. Matching data envelope to color gamut.

Choose the section of the UCS gamut including the  $L^*$  axis that has the best fit to the data. The first two data space vectors will lie parallel to the plane  $\xi = 0$  for some rotation angle  $\phi$ , where

$$\begin{pmatrix} \xi \\ \eta \end{pmatrix} = \begin{pmatrix} \cos \phi & -\sin \phi \\ \sin \phi & \cos \phi \end{pmatrix} \begin{pmatrix} a^* \\ b^* \end{pmatrix}$$

Points 1 and 2 in figure 6.1 are to be put into coincidence by scale, rotation, and bias.

$$\begin{pmatrix} L^* \\ \eta \end{pmatrix}_i = s \begin{pmatrix} \cos \theta & -\sin \theta \\ \sin \theta & \cos \theta \end{pmatrix} \begin{pmatrix} v_1 - b_1 \\ v_2 - b_2 \end{pmatrix}_i \quad i = 1, 2 \quad (6.2)$$

Two solutions for  $(s, \theta, b_1, b_2)$  are permitted, being reflections (in the plane) through the line joining points 1 and 2. Choose the one

giving the desired orientation. If the algorithm used gives only one solution to equation (6.2) and it is the reflection of the one desired, interchange the rows or columns of the  $2 \times 2$  matrix or the elements of either of the vectors, and rerun the algorithm. Now  $x_3$  is laid onto  $\xi$  by

$$\xi = \pm s(v_3 - b_3)$$

with the choice of sign affecting the value of  $b_3$ . The complete transformation is

$$\begin{pmatrix} L^* \\ a^* \\ b^* \end{pmatrix} = s \begin{pmatrix} \cos \theta & -\sin \theta & 0 \\ \sin \phi \sin \theta & \sin \phi \cos \theta & \pm \cos \phi \\ \cos \phi \sin \theta & -\cos \phi \cos \theta & \mp \sin \phi \end{pmatrix} \begin{pmatrix} v_1 - b_1 \\ v_2 - b_2 \\ v_3 - b_3 \end{pmatrix} \quad (6.3)$$

An isoluminous color product (hereinafter referred to as UCS-3) is obtained by taking two-dimensional numerical data and matching the data plane to a constant- $L^*$  plane in color space. The general form of the transformation is

$$\begin{pmatrix} L^* \\ a^* \\ b^* \end{pmatrix} = s \begin{pmatrix} b_3 & 0 & 0 \\ 0 & \cos \theta & \sin \theta \\ 0 & -\sin \theta & \cos \theta \end{pmatrix} \begin{pmatrix} 1/s \\ v_1 - b_1 \\ v_2 - b_2 \end{pmatrix}$$

The isoluminous product will have the same psychophysical brightness everywhere, and information will be exhibited as chromatic displays.

A type of color product that is of interest to the community looking at agriculture is one in which soils are gray and vegetation cover causes a chromatic departure from gray. A drawback to the product (UCS-4) is the reduction in chromatic contrast--the factor  $s$  in equation (6.1)--over what is available with a better geometric fit between data scatter envelope and color gamut. Kauth and Thomas (1977) describe the tasseled cap diagram, of whose features only the green arm and the line of soils interest us here. The tasseled cap is a plot in the plane of

two specific orthogonal linear combinations of the Landsat MSS measurement components. Most of the variability of Landsat's MSS data lies in that plane. As points on cultivated ground move through a cycle of emergence, maturity, harvest, and back to bare ground, they trace out a pattern resembling a tasseled cap. They begin on the line of soils, move to the green arm, and end again on the line of soils. The line of soils is placed into conjunction with the  $L^*$  axis in UCS-4 (fig. 6.2); the form of the transformation is

$$\begin{pmatrix} L^* \\ a^* \\ b^* \end{pmatrix} = s \begin{pmatrix} 1 & 0 & 0 \\ 0 & \cos \theta & \sin \theta \\ 0 & -\sin \theta & \cos \theta \end{pmatrix} \begin{pmatrix} KB - b_1 \\ KG - b_2 \\ KY - b_3 \end{pmatrix}$$

with  $KB$ ,  $KG$ , and  $KY$  being the brightness, green stuff, and yellow stuff, respectively. Determination of the elements  $(\theta, b_1, b_2, b_3)$  is performed as for equation (6.3).

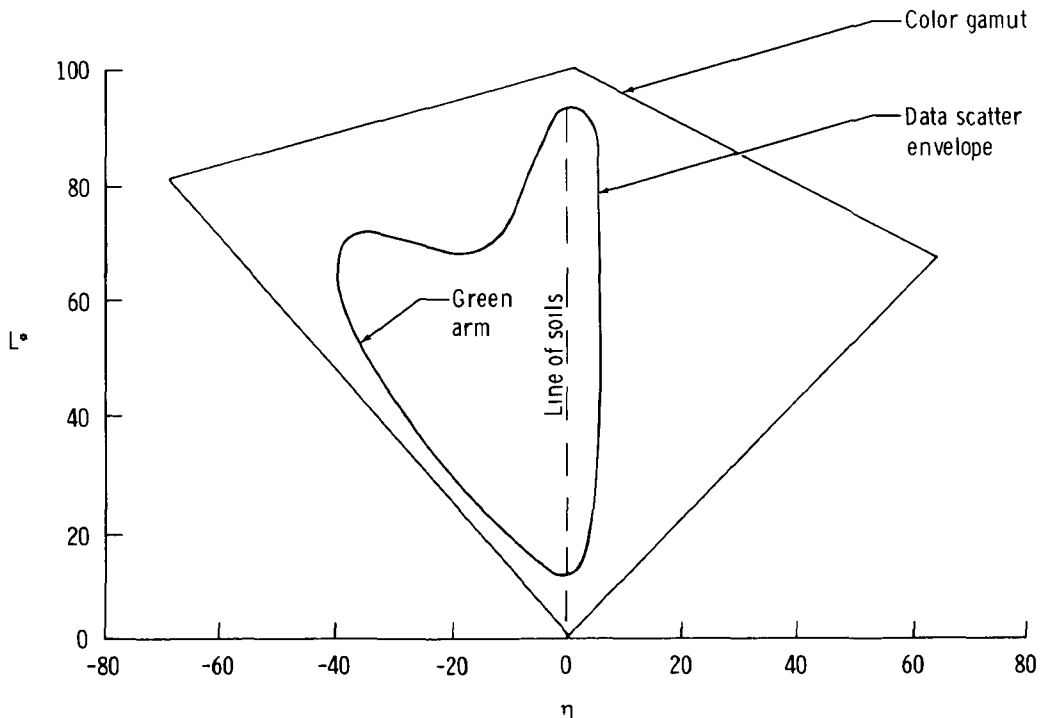


Figure 6.2. Product UCS-4, in which the line of soils is coincident with the gray axis and development of vegetation canopy is in the negative- $\eta$  chromatic direction. Note the unused, but accessible, portion of color space in the positive- $\eta$  direction.

**Page intentionally left blank**

**Page intentionally left blank**

7. NUMERICAL VALUES IN THE PROJECTION-ADDITION  
MODEL FOR THE JOHNSON SPACE CENTER  
FR-80

The measurements of the quantities in the projection-addition model, the derivation of the color gamut for the model, the fitting of particular numerical data within the gamut, and the programming of the algorithms developed by the author were performed by others under the author's guidance. The author vouches for the accuracy of the results but does not feel it appropriate to include the body of the computations. The procedure for adapting the model to an arbitrary film or television system is clear from the material contained here. Numerical examples and the complete description of the Johnson Space Center model FR-80 under the projection-addition model are contained in this section.

As mentioned earlier, the film processing and the light table used for illumination of the transparencies form integral parts of the color generation system. The film processing is regarded as a stable part of the counts-to-integral-spectral-density process, and the light table's spectral radiance is included in tables 7-1 and 7-2.

The density created by singly activating each primary at all 256 levels on a patch of film was shown by microdensitometry to be quite well linearized with respect to control input. Table 7-3 gives the parameters of the lines fit through the data.

Chromaticities of the light table and of the film primaries are calculated in the indicated fashion from tables 7-1 and 7-2. The results are given in the tables. Note that to have absolute values for the tristimulus values, absolute spectral radiance must be used. The chromaticities  $x$  and  $y$  do not depend on absolute calibration. Table 7-4 gives the tristimulus values derived by equations (4.2) and (4.3) for use in the colorimetric model.

The activation vector in the model is calculated using table 7-3 and equations (4.4) through (4.6). Table 7-5 gives the elements of  $(PE)^{-1}$  for use with equation (4.7), which inverts the counts to color process.

Table 7-6 gives the conversion between the  $(L^*a^*b^*)$  approximation to UCS space and tristimulus values  $X, Y, Z$ .

TABLE 7-1

CALCULATION OF LIGHT TABLE CHROMATICITY COORDINATES

[Columns are wavelength, tristimulus distribution coefficients, and relatively (not absolutely) calibrated spectral radiance.]

$\lambda$	$\bar{x}$	$\bar{y}$	$\bar{z}$	$E_\lambda$
410	0.0143	0.0004	0.0679	1.105
420	.0435	.0012	.2074	.931
430	.1344	.0040	.6456	2.192
440	.2839	.0116	1.3856	6.063
450	.3483	.0230	1.7471	2.891
460	.3362	.0380	1.7721	2.530
470	.2908	.0600	1.6692	2.892
480	.1954	.0910	1.2876	2.865
490	.0956	.1390	.8130	2.782
500	.0320	.2080	.4652	3.072
510	.0049	.3230	.2720	2.889
520	.0093	.5030	.1582	3.003
530	.0633	.7100	.0782	3.392
540	.1655	.8620	.0422	4.141
550	.2904	.9540	.0203	7.628
560	.4334	.9950	.0087	8.140
570	.5945	.9950	.0039	8.570
580	.7621	.9520	.0021	8.694
590	.9163	.8700	.0017	7.699
600	1.0263	.7757	.0011	7.424
610	1.0622	.6310	.0008	6.058
620	1.0026	.5030	.0003	5.019
630	.8544	.3810	.0002	3.790
640	.6424	.2650	.0000	2.783
650	.4479	.1750	.0000	2.173
660	.2835	.1070	.0000	1.617
670	.1649	.0610	.0000	1.192
680	.0784	.0320	.0000	1.362
690	.0468	.0170	.0000	.667
700	.0227	.0082	.0000	.513
710	.0114	.0041	.0000	.495
720	.0058	.0021	.0000	.363
730	.0029	.0010	.0000	.374
740	.0014	.0005	.0000	.359
750	.0007	.0003	.0000	.294
760	.0003	.0001	.0000	.301

$$X_0 = \sum_i \bar{x}(\lambda_i) \cdot L_\lambda(\lambda_i)$$

$$Y_0 = \sum_i \bar{y}(\lambda_i) \cdot L_\lambda(\lambda_i)$$

$$Z_0 = \sum_i \bar{z}(\lambda_i) \cdot L_\lambda(\lambda_i)$$

$$x = \frac{X}{X + Y + Z}$$

$$y = \frac{Y}{X + Y + Z}$$

$$x_0 = 0.3684$$

$$y_0 = 0.4131$$

TABLE 7-2

CALCULATION OF CHROMATICITY COORDINATES FOR THE THREE FILM PRIMARIES

[Columns are wavelength, tristimulus distribution coefficients, relative spectral radiance of light table, and wavelength-dependent transmission of fully activated film primaries.]

$\lambda$	$\bar{x}$	$\bar{y}$	$\bar{z}$	$E\lambda$	$\tau_G$	$\tau_B$	$\tau_R$
400	0.0143	0.0004	0.0679	1.105	0.020	0.080	0.000
410	.0435	.0012	.2074	.931	.020	.092	.000
420	.1344	.0040	.6456	2.192	.016	.107	.000
430	.2839	.0116	1.3856	6.063	.014	.116	.000
440	.3483	.0230	1.7471	2.891	.015	.139	.000
450	.3362	.0380	1.7721	2.530	.016	.165	.000
460	.2908	.0600	1.6692	2.829	.020	.175	.000
470	.1954	.0910	1.2876	2.865	.028	.170	.000
480	.0956	.1390	.8130	2.782	.047	.145	.000
490	.0320	.2080	.4652	3.072	.079	.110	.000
500	.0049	.3230	.2720	2.889	.115	.074	.000
510	.0093	.5030	.1582	3.003	.151	.045	.000
520	.0633	.7100	.0782	3.392	.190	.028	.005
530	.1655	.8620	.0422	4.141	.207	.018	.005
540	.2904	.9540	.0203	7.628	.198	.013	.015
550	.4334	.9950	.0087	8.140	.176	.010	.035
560	.5945	.9950	.0039	8.570	.155	.010	.074
570	.7621	.9520	.0021	8.694	.134	.010	.115
580	.9163	.8700	.0017	7.699	.116	.010	.150
590	1.0263	.7757	.0011	7.424	.093	.015	.172
600	1.0622	.6310	.0008	6.058	.071	.012	.182
610	1.0026	.5030	.0003	5.019	.051	.011	.187
620	.8544	.3810	.0002	3.790	.037	.010	.188
630	.6424	.2650	.0000	2.783	.026	.000	.190
640	.4479	.1750	.0000	2.173	.021	.000	.193
650	.2835	.1070	.0000	1.617	.019	.000	.205
660	.1649	.0610	.0000	1.192	.016	.000	.218
670	.0874	.0320	.0000	1.362	.014	.000	.218
680	.0468	.0170	.0000	.667	.013	.000	.218
690	.0227	.0082	.0000	.513	.013	.000	.218
700	.0114	.0041	.0000	.495	.015	.000	.218
710	.0058	.0021	.0000	.363	.018	.000	.218
720	.0029	.0010	.0000	.374	.018	.000	.218
730	.0014	.0005	.0000	.359	.018	.000	.218
740	.0007	.0003	.0000	.294	.018	.000	.218
750	.0003	.0001	.0000	.301	.018	.000	.218

$$X_j = \sum_1 \bar{x}(\lambda_i) L_\lambda(\lambda_i) \tau_j(\lambda_i), \quad j = \text{green, blue, red.}$$

Similar expressions for  $Y_j, Z_j$  (see table 7-1).

	Green	Blue	Red
x	0.3603	0.1919	0.5529
y	0.5730	0.1540	0.4458

TABLE 7-3

LINEAR FIT TO FILM DENSITY VS. INPUT COUNTS

Film Primary	Maximum Density (zero counts)	Minimum Density (255 counts)
Red	2.520	0.753
Green	2.182	.306
Blue	2.513	.694

TABLE 7-4

TRISTIMULUS VALUES OF LIGHT TABLE AND FULLY  
ACTIVATED INDIVIDUAL PFC CHANNELS

$\begin{pmatrix} X_0 & X_R & X_G & X_B \\ Y_0 & Y_R & Y_G & Y_B \\ Z_0 & Z_R & Z_G & Z_B \end{pmatrix}$	=	$\begin{pmatrix} 89.18 & 39.74 & 35.90 & 13.53 \\ 100 & 32.04 & 57.09 & 10.46 \\ 52.89 & .09343 & 6.646 & 46.13 \end{pmatrix}$
---	---	--

TABLE 7-5

MATRIX ELEMENTS FOR EQUATION (4.7), THE INVERSION  
FROM COLOR SPACE TO INPUT COUNTS

---



---


$$PE = \begin{pmatrix} 0.1198 & 0.2359 & 0.04152 \\ .09657 & .3751 & .03210 \\ .0002816 & .04366 & .1415 \end{pmatrix}$$

$$(PE)^{-1} = \begin{pmatrix} 16.47 & -10.05 & -2.548 \\ -4.349 & 5.395 & .05223 \\ 1.309 & -1.645 & 7.056 \end{pmatrix}$$


---

TABLE 7-6

## CONVERSION BETWEEN (L\*a\*b\*) AND (X,Y,Z)

---

Let the reference illumination yield tristimulus values  $X_0$ ,  $Y_0$ ,  $Z_0$  when put at normal incidence onto a perfectly diffuse, perfectly reflecting surface. The relationship, for an arbitrary reflecting object, between its tristimulus values and its (L\*a\*b\*) coordinates is given by the CIE (1976) as

$$L^* = 25 \left( 100 \frac{Y}{Y_0} \right)^{\frac{1}{3}} - 16, \quad 1 \leq Y \leq 100$$

$$a^* = 500 \left[ \left( \frac{X}{X_0} \right)^{\frac{1}{3}} - \left( \frac{Y}{Y_0} \right)^{\frac{1}{3}} \right]$$

$$b^* = 200 \left[ \left( \frac{Y}{Y_0} \right)^{\frac{1}{3}} - \left( \frac{Z}{Z_0} \right)^{\frac{1}{3}} \right]$$

Given the reference illumination tristimulus values,

$$Y = Y_0 \frac{(L^* + 16)^3}{1562500}$$

$$X = X_0 \left[ \frac{a^*}{500} + \left( \frac{Y}{Y_0} \right)^{\frac{1}{3}} \right]$$

$$Z = Z_0 \left[ \left( \frac{Y}{Y_0} \right)^{\frac{1}{3}} - \frac{b^*}{200} \right]$$


---

## 8. IMAGERY PRODUCED BY UCS TRANSFORMATIONS

The accompanying color images are a set made under the UCS-1 and UCS-2 transformations. The three coordinates employed are the tasseled cap (Kauth and Thomas, 1977) brightness, greenness, and yellowness. The suppressed dimension carries very little variance. The net effect is that one linear combination of the four Landsat MSS channels is suppressed, and that the eye is directly viewing the remaining three dimensions, since the tasseled cap transformation is a rotation matrix.

The color plates are positive prints made from transparencies. Some color fidelity has been lost, and color relationships will be modulated by the local illumination. However, the general character has been retained. The author will attempt to provide transparencies in response to appropriate requests. Note well that the relationship between control input and color output for such transparencies is particularized to a combination of machine, film, development chemistry, and viewing illumination. The measurements outlined in section 4 are required to permit duplication of results on another system. Once that has been done, though, near-identical color pictures should be producible on disparate machines--even CRT and film displays.

In UCS-1, individual scenes have their scatter plots fit to the color space; in UCS-2, an envelope is fit. As a result, UCS-1 has high chromatic contrast, and UCS-2 has a stability in the counts-to-colors process. The numerical data were corrected for sun angle by ratio of solar zenith angle cosines. The same rotation matrix  $R$  in equation (6.1) is used; UCS-1 and UCS-2 differ only in scale and bias.

A single area on the ground, approximately five by six miles, is presented at four times under the two transformations.

At the stage in the project at which these images were generated, the algorithm to handle saturated picture elements had not been fully settled. The occasional saturated picture elements in this imagery are glaringly out of context, either yellow or red. Good chromatic contrast is apparent, and this is achieved with few picture elements saturating.

Wallis (1975, sec. 3.2) discusses the manner of displaying a picture element whose desired color falls outside the color gamut. He suggests displaying the gamut color that is closest (when measured in a UCS space) to the desired color. If the color space is regarded as having the drive signals of the color primaries as basis vectors, a zero-one clamp is appropriate by his criterion. This author suggests that other criteria can be formulated using the framework of angularity developed in section 3. The proposed criterion for treating a picture element logically falling outside the gamut is to display the gamut boundary

color associated with the angularity of the problem picture element. In this fashion, lightness, for what will be the most common example, will not be properly displayed for a saturating picture element, but the element's chromatic properties will be maintained. Unless the gamut boundary can be analytically expressed, an iterative technique would be required to find the appropriate color. A noniterative approximation to the criterion was adopted in producing imagery later in the project; the drive signals calculated for the desired color were reduced in proportion so that the largest drive signal was just at saturation. The method is illustrated in figure 8.1. All drive signals were set to zero for a picture element which had any drive channel that saturated below zero; in practice there were very few of these. This criterion seemed preferable to a zero-one clamp on individual channels; picture elements that were treated by the earlier method with visually jangling results were noticeably more at peace with their neighbors when transformed into color by the later approximation.

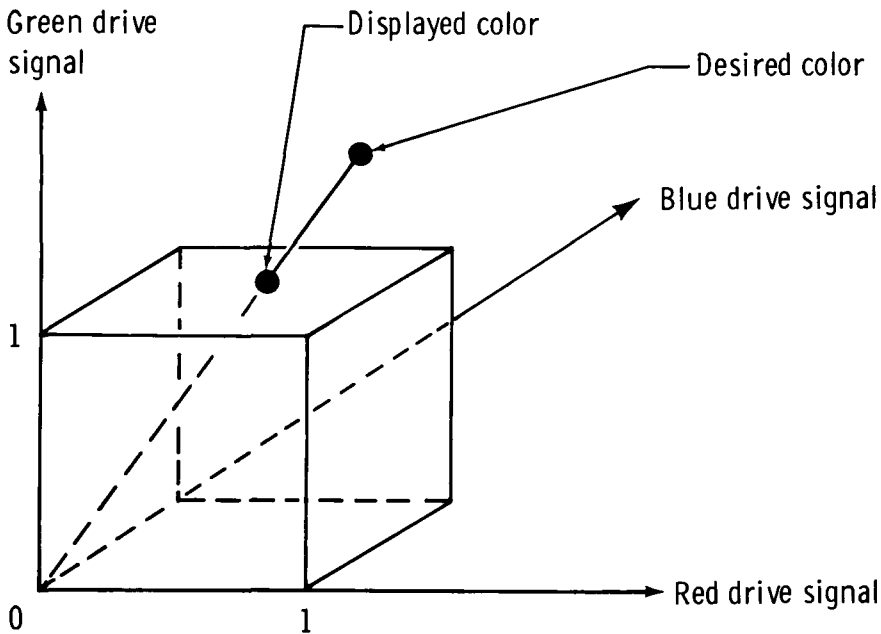


Figure 8.1. Method used to display a saturated color.

The scale factor (colors per count) is uniformly higher in UCS-1 than in UCS-2. The example imagery had the following scale factors:

<u>Date</u>	<u>UCS-1</u>	<u>UCS-2</u>
75/311	2.63	0.76
76/018	3.7	.76
76/162	1.61	.76
76/198	1.11	.76

The very high value for the 76/018 UCS-1 product is responsible for the speckled appearance; the noise level has been blown up to the point of visibility.

The chromatic balance is oriented so that green vegetation is toward magenta, the line of soils toward green. The majority of variance present in the data is in the green vs. magenta, light vs. dark plane. In UCS-2, data motions perpendicular to that plane are visible as an overall shift (toward brownish in the fall and winter scenes) in the chromatic appearance.

Two reasons underlie the particular choice of chromatic orientation, that healthy vegetation is magenta (in contrast to conventional false-color imagery, in which vegetation is red). Primarily, the color gamut in UCS coordinates has the largest cross section in the green/magenta, light/dark plane. Fitting the essentially planar MSS data to that section allowed the largest chromatic expansion with little saturation. Secondly, having vegetation be magenta rather than red forces the analyst to develop a new set of color interpretations. The author feels the UCS imagery is of a sufficiently different character than conventional imagery that it is inadvisable to carry over interpretations.

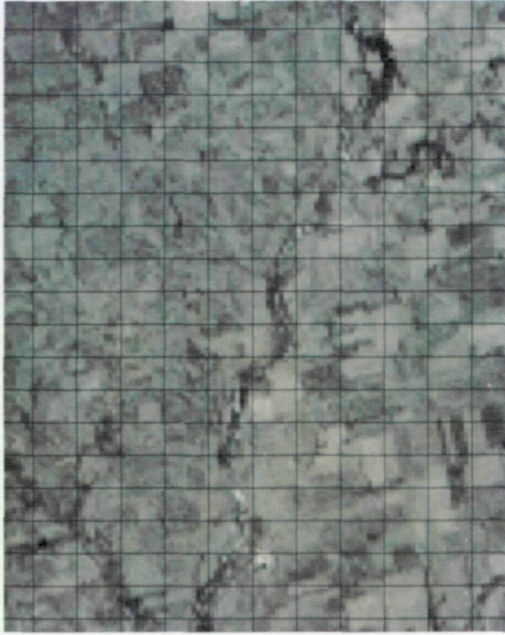
The imaged area is a winter wheat agricultural area of North Dakota. In the fall data, emergent wheat is visible as the purplish fields. Dormancy follows with less distinction between wheat and other. In the spring, the emerged wheat is seen to move more rapidly toward the bright magenta of full healthy vegetation cover than do other fields. In the final acquisition, harvested fields are bright and near achromatic. The UCS-1 images quite apparently do not have the consistency of color keys as the UCS-2. However, the eye has no difficulty relating the two images from the same acquisition; the same chromatic directions of motion result in the similar appearance. The viewer has no difficulty in interpreting corresponding UCS-1 and UCS-2 images as having similar directions, just differing offsets and contrasts.

Examples of the color imagery are shown on plates 1 and 2. Images A, C, E, and G are high-chromatic-contrast images; B, D, F, and H have a constant relationship between sun-angle-corrected data and color. Images A and B were acquired on November 8, 1975 (emergent winter wheat is purplish). Images C and D were acquired during dormancy (January 18, 1976). Images E and F are from June 15, 1976, with fields well along in development. Images G and H are at maturity (July 17, 1976), with harvested fields being a light cream and mature crops an intense purple.

The following features appear, in consonance with characteristics of the numerical data. Essentially, only two color dimensions (light/dark and green/magenta) are present in any one image. A seasonal shift (toward brown in winter) is visible in UCS-2, the constant-transformation product. The chromatic sense of variations within a scene is identical on any date; the chromatic contrast is higher in UCS-1.

These images were made using a zero-one clamp to show a saturated pixel. Good chromatic expansion with few saturated pixels is evident.

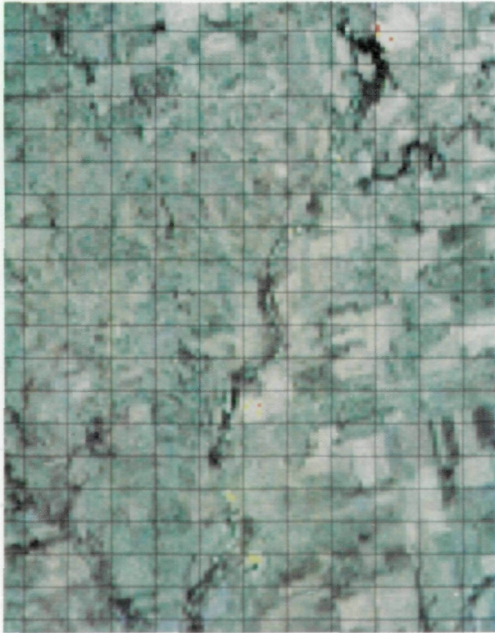
There is an inevitable loss of chromatic contrast resulting from the fact that the color pictures in these two plates are two generations removed from the original color-controlled transparencies.



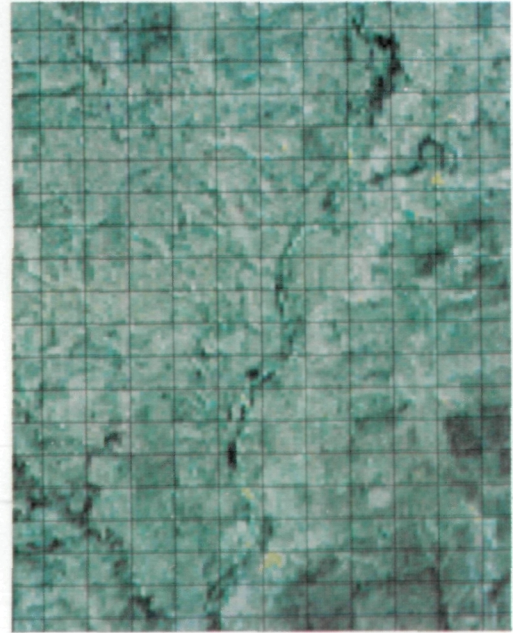
B



D

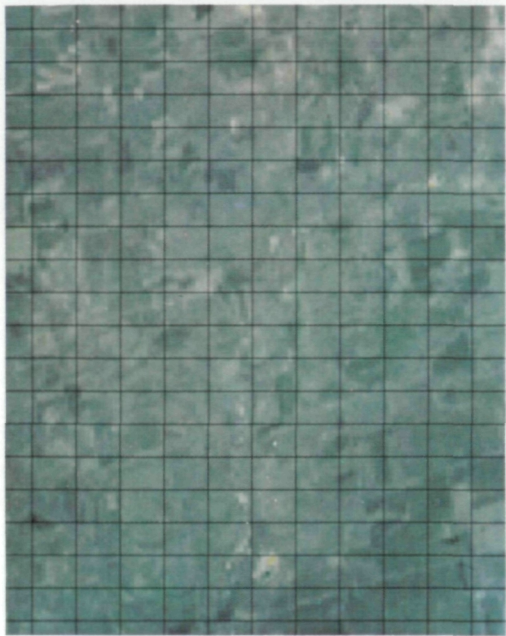


A

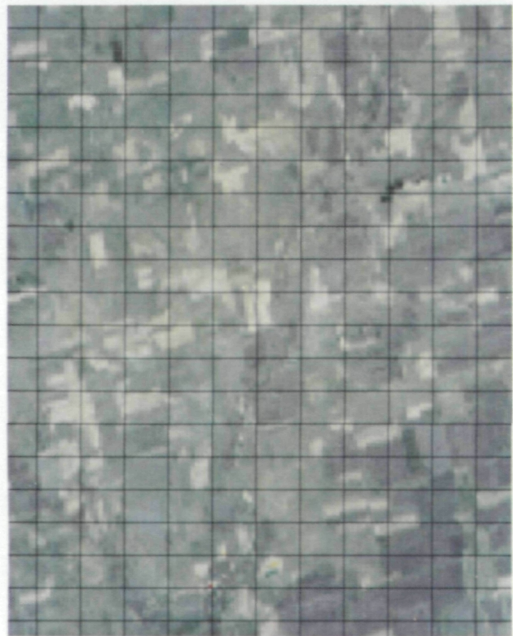


C

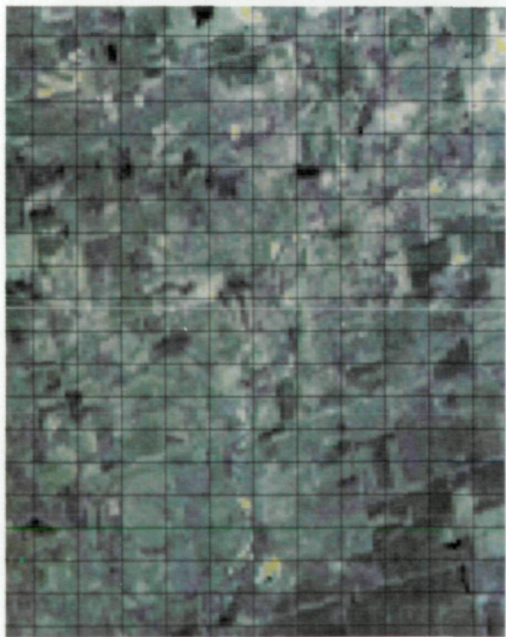
PLATE 1



F



H



E



G

PLATE 2

## 9. CONCLUSIONS

The author opines that the UCS character of the imagery is indicated and that numerical control of color generation, to at least first order, is achieved.

Further work to be done includes applying the  $(\mathcal{L}, j, g)$  system, which will require an iterative or table lookup inversion. The  $(L^*a^*b^*)$  system will be subjected to close scrutiny and its imagery given a competitive comparison with previously existing film products. The author hopes that a single UCS transformation may be sufficiently economical in its use of the accessible portions of color space that the UCS product can supplant two or three standard products (high contrast, color fidelity, and reverse polarity) currently in use to show analysts at the Johnson Space Center various aspects of numerical imagery. If the UCS imagery shows practical promise, the accuracy of the projection-addition model will be tested and perhaps improved as indicated. Finally, the existing inversion routine may be replaced by a single, high-speed, table lookup method of getting from colors to control inputs.

**Page intentionally left blank**

**Page intentionally left blank**

## ABBREVIATIONS AND SYMBOLS

### ABBREVIATIONS :

CIE	Commission Internationale de l'Eclairage, the International Illumination Committee
CRT	cathode-ray tube
END	equivalent neutral density
H&D	Hurter and Driffield; refers to a plot of transmission density vs. log exposure for a photographic emulsion
JND	just noticeable difference, the unit of detectable color difference
MSS	multispectral scanner
PFC	production film converter
UCS	uniform chromaticity scale

SYMBOLS :

$\underline{a} = \begin{pmatrix} a_R \\ a_G \\ a_B \end{pmatrix}$	Vector representation of activation in all PFC channels
$a_j$	Activation of a PFC channel, the ratio $\tau/\tau_{\max}$ for that channel
$b_i$	Bias in the i-th data channel; element of the bias vector $\underline{b}$
$c, m, y$	Respectively the cyan, magenta, and yellow dyes' END's; as subscripts, pertaining to cyan, magenta, and yellow dyes
$D$	Transmission density, $D = \log_{10} \tau$ ; herein referred to as "density"
$\mathcal{D}$	Set of integral spectral densities $\{D(\lambda, \underline{J}_i)\}$ produced from the members of $\mathcal{J}$
$E$	Irradiance [watts $\cdot$ m $^{-2}$ ]
$\mathbb{E}$	A $3 \times 3$ diagonal matrix of minimum transmission values
$E_\lambda$	Spectral irradiance [watts $\cdot$ m $^{-2}\cdot$ nm $^{-1}$ ]
$e$	Spectral analytical dye density
$f$	A fraction, $0 \leq f \leq 1$
$\mathcal{U}$	Grid of color vectors $\underline{U}_i$ corresponding to $\mathcal{J}$
$h$	A normalizing constant
$i$	Index; has varying domain given in context
$\mathcal{J}$	Grid of control vectors $\underline{J}_i$ corresponding to $\mathcal{U}$
$J_j$	Input counts in the j-th PFC channel
$j$	Index varying over R, G, B, and sometimes 0
$\underline{K} = \begin{pmatrix} K_C \\ K_M \\ K_Y \end{pmatrix}$	Density of unexposed film, measured for the cyan, magenta, and yellow dyes

KB,KG,KY	The first three tasseled cap components (Kauth and Thomas, 1977); they are mutually orthogonal linear combinations of Landsat MSS channels and contain most of the MSS variance
k	Index varying over c, m, y
$\bar{L}$	Radiance [ $\text{watts} \cdot \text{m}^{-2} \cdot \text{ster}^{-1}$ ]
$\mathcal{L}, j, g$ $L^*, a^*, b^*$	Coordinates in approximations to a uniform chromaticity scale space
$L_\lambda$	Spectral radiance [ $\text{watts} \cdot \text{m}^{-2} \cdot \text{ster}^{-1} \cdot \text{nm}^{-1}$ ]
m	Number of data points; also, magenta dye density
n	Number of channels in a data vector
P	A distribution function
$\mathbb{P}$	A $3 \times 3$ matrix of tristimulus values for full activation of primaries
$\underline{q}(\underline{J})$	A vector having for components $q_j$ raised to the $J_j$ power
$q_j$	In the $j$ -th PFC channel, the 255th root of the ratio of maximum to minimum transmission
R,B,G	As subscripts, referring to the red, blue, and green channels in the PFC
$\mathbb{R}$	A $3 \times 3$ rotation matrix
s	Chromatic expansion factor, having dimensions [ $\text{JND}'\text{s} \cdot \text{count}^{-1}$ ]
$\underline{T} = \begin{pmatrix} X \\ Y \\ Z \end{pmatrix}$	Vector representation of tristimulus values
$\underline{t}(\lambda) = \begin{pmatrix} \bar{x}(\lambda) \\ \bar{y}(\lambda) \\ \bar{z}(\lambda) \end{pmatrix}$	Vector representation of tristimulus distribution coefficients
$\underline{U} = \begin{pmatrix} L^* \\ a^* \\ b^* \end{pmatrix}$	Vector representation of UCS coordinates

UCS-1,-2,-3,-4	Film transparencies produced by four algorithms relating data vectors to color vectors; also, the algorithms themselves
$\underline{v}$	Data vector, having components $v_1, v_2, \dots, v_n$
X,Y,Z	Standard CIE tristimulus values
$X_0, Y_0, Z_0$	Tristimulus values for a reference illumination
x,y,z	Chromaticity coordinates (y is also yellow dye density)
$\bar{x}(\lambda), \bar{y}(\lambda),$	Tristimulus distribution coefficients
$\bar{z}(\lambda)$	
0	As a subscript, referring to the reference illumination
$\Upsilon_{kj}$	The elements of $\Pi$
$\Pi$	A $3 \times 3$ interimage sensitivity matrix
$\Delta$	Difference; also, Maxwell triangle
$\underline{\Delta}$	A vector difference
$\theta, \phi$	Rotation angles
$\lambda$	Wavelength; as a subscript, implies partial derivative with respect to wavelength
$\xi, \eta$	Rotations of the UCS parameters $a^*$ and $b^*$
$\tau$	Transmittance factor (referred to herein as "transmission"); ratio of flux transmitted and detected, for a physical sample and an idealized reference
$\int_{\lambda}$	Integral performed over the wavelength range where non-zero tristimulus distribution coefficients exist

## REFERENCES

- CIE. 1976. Agreements reached by the Committee. Appendix 2. Compte rendu 18<sup>e</sup> session. CIE n<sup>o</sup> 36, p. 171. Paris.
- Eynard, Raymond A., ed. 1973. Color: theory and imaging systems. Washington: Society of Photographic Scientists and Engineers.
- Faugeras, Olivier Dominique. 1976. Digital color image processing and psychophysics within the framework of a human visual model. University of Utah report UTEC-CSc-77-029. Available through the National Technical Information Service, Springfield, Virginia, as order number N77-29742.
- Friele, L. F. C. 1972. A survey of some current color difference formulae. In Color metrics. AIC/Holland, Soesterberg.
- General Electric. n.d. ERTS reference manual. Philadelphia: Valley Forge Space Center.
- Judd, Deane B., and Wyszecki, Gunter. 1963. Color in business, science, and industry. New York: Wiley.
- Kauth, R. J., and Thomas, G. S. 1977. The tasselled cap--a graphic description of the spectral-temporal development of agricultural crops as seen by Landsat. In Proceedings of the 1976 Machine Processing of Remotely Sensed Data Symposium. West Lafayette, Indiana: Purdue University.
- Kullback, Solomon. 1968. Information theory and statistics. New York: Dover.
- Lambeck, Peter F., Kauth, Richard, and Thomas, Gene S. 1978. Data screening and preprocessing for Landsat MSS data. In Proceedings of the 12th international symposium on remote sensing of environment. Ann Arbor: Earth Resources Institute of Michigan.
- MacAdam, David L. 1967. Color science and color photography. Physics Today 20:27-39.
- \_\_\_\_\_. 1974. Uniform color scales. J. Opt. Soc. Am. 64:1691-1702.
- \_\_\_\_\_. 1942. Visual sensitivities to color differences in daylight. J. Opt. Soc. Am. 32:247.

- McCamy, C. S. 1973. Color densitometry. In Color: theory and imaging systems. Washington: Society of Photographic Scientists and Engineers.
- Nimeroff, I. 1968. Colorimetry. National Bureau of Standards Monograph 104. Washington: U.S. Government Printing Office.
- Pearson, Milton. 1973. Masking and color reproduction. In Color: theory and imaging systems. Washington: Society of Photographic Scientists and Engineers.
- Polger, John E. 1973. Generation of color imagery from Earth Resources Technology Satellite (ERTS) data return. In Color: theory and imaging systems. Washington: Society of Photographic Scientists and Engineers.
- Pratt, William K. 1978. Digital image processing. New York: Wiley.
- Sanderson, T. W. 1958. An introduction to multivariate statistical analysis. New York: Wiley.
- Scarpace, Frank L. 1978. Densitometry on multi-emulsion imagery. In Photogrammetric engineering and remote sensing. 44:1279.
- \_\_\_\_\_, and Friedrichs, G. A. 1978. A method of determining spectral analytical dye densities. In Photogrammetric engineering and remote sensing. 44:1293.
- Taylor, M. M. 1974. Principal components colour display of ERTS imagery. In Proceedings of the second Canadian symposium on remote sensing. Guelph: University of Guelph.
- Wallis, R. H. 1975. Film recording of digital color images. University of Southern California Image Processing Institute report 570, 201 pp. Available through the National Technical Information Service, Springfield, Virginia, as order number N77-78922.
- Wyszecki, Gunter, and Stiles, W. S. 1967. Color science: concepts and methods, quantitative data and formulas. New York: Wiley.

1 Report No NASA TM-58215		2 Government Accession No		3 Recipient's Catalog No	
4 Title and Subtitle  COLORIMETRIC PRINCIPLES AS APPLIED TO MULTICHANNEL IMAGERY				5 Report Date July 1979	
				6 Performing Organization Code JSC-14873	
7 Author(s) Richard D. Juday				8 Performing Organization Report No	
9 Performing Organization Name and Address  Lyndon B. Johnson Space Center Houston, Texas 77058				10 Work Unit No 658-89-00-00-72	
				11 Contract or Grant No	
				13 Type of Report and Period Covered Technical Memorandum	
12 Sponsoring Agency Name and Address  National Aeronautics and Space Administration Washington, D.C. 20546				14 Sponsoring Agency Code	
15 Supplementary Notes Presented as a thesis to the faculty and staff of the School of Sciences and Technologies, the University of Houston at Clear Lake City, in partial fulfillment of the requirements for the degree of Master of Science in Physical Sciences.					
16 Abstract  The objective of this work is the false-color display of numerical multichannel imagery so that the viewer of the imagery perceives in proportion the significant relationships present in the numerical imagery. The first part of the problem is extracting the significant features in the multichannel imagery while reducing dimensionality to no more than three independent quantities. The second part is modeling the colorimetry of the color image generating machinery, relating the color output as measured in a uniform chromaticity scale (UCS) space to the control input. The third part is determining a linear, orthogonal transformation between the occupied portions of the data space and the UCS space attainable by the color image machine. Mathematical inversion of the relationship from input to color then yields the control vector to apply to the color machine. The principles behind the extraction of significant features and dimensionality reduction are discussed. Some apropos qualities in multispectral scanner data are described, and some transformations that leave them invariant are given. A simple invertible color model and its supporting measurements are described for a computer-driven CRT-to-film image generating machine. Examples of color imagery produced from Landsat data are evaluated, and further work is outlined.					
17 Key Words (Suggested by Author(s)) Color                      Uniform chromaticity Color image              Colorimetry Multispectral              Numerical imagery Image processing        Remote sensing False color                Landsat				18 Distribution Statement  STAR Subject Category: 43 (Earth Resources)	
19 Security Classif (of this report) Unclassified		20 Security Classif (of this page) Unclassified		21 No of Pages 68	22 Price* \$4.50

\*For sale by the National Technical Information Service, Springfield, Virginia 22161

National Aeronautics and  
Space Administration

Washington, D.C.  
20546

Official Business  
Penalty for Private Use, \$300

THIRD-CLASS BULK RATE

Postage and Fees Paid  
National Aeronautics and  
Space Administration  
NASA-451



3 2 10.E, 070679 S90844HU  
MCDONNELL DOUGLAS CORP  
ATTN: PUBLICATIONS GROUP PR 15246-A  
P O BOX 516  
ST LOUIS MO 63166

**NASA**

POSTMASTER: If Undeliverable (Section 158  
Postal Manual) Do Not Return

10 JAN 1987 *John Syme 852C/220/3M/36159 24 JUN 83*  
MAR 20 1987 *Richard Backe E422/107 A10 13 MAY 87 CT*